Wright State University

CORE Scholar

2022

Covalent Attachment of TADF Chromophores to Thermally Stable Poly(arylene ether)s

Samuel Farrar
Wright State University

Follow this and additional works at: https://corescholar.libraries.wright.edu/etd_all

Part of the Chemistry Commons

COVALENT ATTACHMENT OF TADF CHROMOPHORES TO THERMALLY

STABLE POLY(ARYLENE ETHER)S

A thesis submitted in partial fulfillment of the

requirements for the degree of

Master of Science

by

SAMUEL FARRAR

B.S, Otterbein University, 2020

2022

Wright State University

WRIGHT STATE UNIVERSITY

GRADUATE SCHOOL

06/29/2022

I HEREBY RECOMMEND THAT THE THESIS PREPARED UNDER MY SUPERVISION BY Sam Farrar ENTITLED Covalent Attachment of TADF chromophores to Thermally Stable Poly(arylene ether)s BE ACCEPTED IN PARTIAL FULFILLMENT OF THE REQUIREMENTS FOR THE DEGREE OF Master of Science.

_____
Eric Fossum, Ph.D.
Thesis Director

_____
Audrey McGowin, Ph.D.
Chair, Department of Chemistry

Committee on Final Examination:

_____
Eric Fossum, Ph.D.

_____
Rachel Aga, Ph.D.

_____
David Dolson, Ph.D.

_____
Barry Milligan, Ph.D.
Dean of the Graduate School

Abstract

Farrar, Samuel. M.S., Department of Chemistry, Wright State University, 2022. Covalent Attachment of TADF chromophores to Thermally Stable Poly(arylene ether)s.

The covalent attachment of a blue emitting, benzothiazole based TADF chromophore into poly(arylene ether) backbone polymers was explored. A benzothiazole derivative, 2-(2,4-difluorophenyl)-benzothiazole (2,4-diF-BTZ), was synthesized to form the electrophilic component of the host polymer. Two polymers were synthesized to have chromophore incorporated, using 2,4-diF-BTZ and 4,4-dihydroxydiphenyl ether (DPE) or 4,4'-biphenol (BP). The chromophore was covalently incorporated at a 10% molar ratio into the polymer backbone by copolymerization with 2,4-diF-BTZ and BP, utilizing nucleophilic aromatic substitution (NAS). Structural characterization was provided via NMR spectroscopy and GC/MS analysis. The polymer syntheses provided high molecular weight materials that were able to be cast into somewhat brittle films. The copolymers possessed glass transitions temperatures (T_g) in excess of 200°C. Photophysical analysis of the copolymers revealed the copolymers emitted light in the blue-green region of the visible spectrum, from 400 nm to 550 nm when excited at 365 nm.

Table of Contents

List of Figures

List of Schemes

List of Tables

Acknowledgements

I'd like to acknowledge my advisor, Dr. Eric Fossum, for guiding me through my time at Wright State and sharing his knowledge and experience with me. I would also like to acknowledge the members of my committee, Dr. Rachel Aga, and Dr. David Dolson. I'd like to acknowledge the other members of the Fossum research group, especially Garrett Reinhard, who provided he previously synthesized materials used and the NMR data for those compounds, as well as the Wright State University Department of Chemistry.

I'd like to also acknowledge the group of friends that I made during my time at Wright State for making my time there fun during such a strange point of history. I'd also like to acknowledge the friends I have from Otterbein and from home that supported me and kept me sane as I continued my education.

I'd finally like to acknowledge my family for all the support they gave me throughout my education. To quote my brother, "It's about time".

Introduction

1.1: Lighting the world

Lighting the world is a costly endeavor, in both an energy sense and a monetary sense. Current methods, like incandescent lighting lose approximately 90% of the energy used to generate light as heat and have a lifetime that is only 1000 hours. Incandescent lighting is still one of the most common methods of lighting used. This method of lighting uses a filament, typically made of tungsten, that is heated until it is white hot, leading to the inefficiency and limiting lifespan on the bulbs. In efforts to increase the lifespan of incandescent lights, the halogen bulb was created. The filament in these bulbs is surrounded by gas, and a heat-reflective coating was applied to the interior of the bulb. These bulbs have an increased lifespan between 2000 and 3000 hours, and increased energy efficiency.[1]

Another method that has become common for lighting is fluorescent lighting. Fluorescent lighting, using thin tubes that are filled with an inert gas and a small amount if mercury gas is typically utilized in office spaces or in homes. When a current is applied through the gas, it becomes excited and produces ultra-violet light. The UV light then excites a fluorescent coating on the inside of the tube, which releases visible light. Compared to halogen bulbs, fluorescent

lights are more efficient and have a longer lifespan, using 75% less energy and lasting up to 15000 hours.[1]

As the demand for a more efficient method of lighting grew, there was a rise in the use of light emitting diodes (LEDs) and more recently, organic light emitting diodes (OLEDs). LEDs offer improved efficiency and longer lifespans than incandescent and fluorescent lighting, using 75% less energy than incandescent lighting and lasting between 15000 and 25000 hours. LEDs also find use in displays of screens alongside their use in lighting.[2]

1.2: LEDs

LEDs operate using crystalline, inorganic semiconductors for light generation. The semiconductor has designed impurities, called dopants, which form a junction where the light generation takes place. This junction is called the p-n junction and is made up of two layers, the p-layer, and the n-layer. The p-layer is doped with electron poor dopants, giving it a positive charge. The n-layer is doped with electron rich dopants, giving it a negative charge. These layers are between an anode and a cathode, resulting in a one-way flow of electrons through the semiconductor. When a voltage is applied to the semiconductor, electrons flow from the n-layer to the p-layer. This forms holes in the n-layer, which then move back and forth between the layers as the electrons flow. When used in lighting, the semiconductor is attached to a reflective cup, which redirects the generated light out the front of the device.[3]
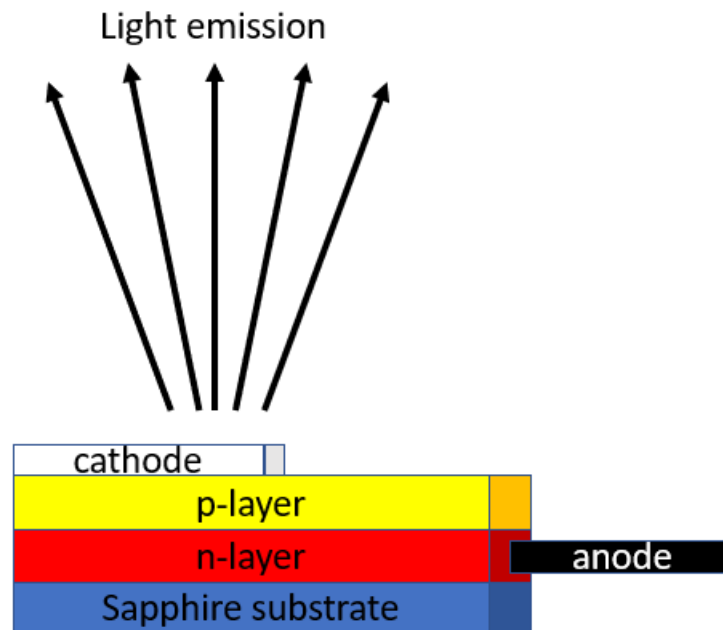
Figure 1: Structure of a LED

Despite their improved efficiencies and lifespans, there are draw backs to using LEDs: they are brittle due to the metals used in the p-n junction, uncommon and costly to use. One of the most common metals used for semiconductors in LEDs is indium, which has an abundancy of 0.1 parts per million in the Earth's crust. The rarity of these components drives the cost of LEDs up. The brittle nature of the p-n junction also makes LEDs inflexible and not suited for use in larger or non-planar displays.[3]

1.3: OLEDs

Recently, OLEDs have begun to appear in lighting and in display applications. Like LEDs, OLEDs are composed of two layers, the hole transport layer and the electron transport layer, sandwiched between an anode and a

cathode. These layers take the place of the p-layer and the n-layer respectively. When a voltage is applied to the OLED, electrons will flow from the anode to the electron transport layer and hole will begin to flow from the hole transport layer to the cathode. The layer where the holes and the electrons meet is called the emissive layer and can be either transport layer or a completely separate layer. The recombination of the holes and the electrons in the emissive layer excites the chromophore in the OLED, which then produces the observed light.[4]
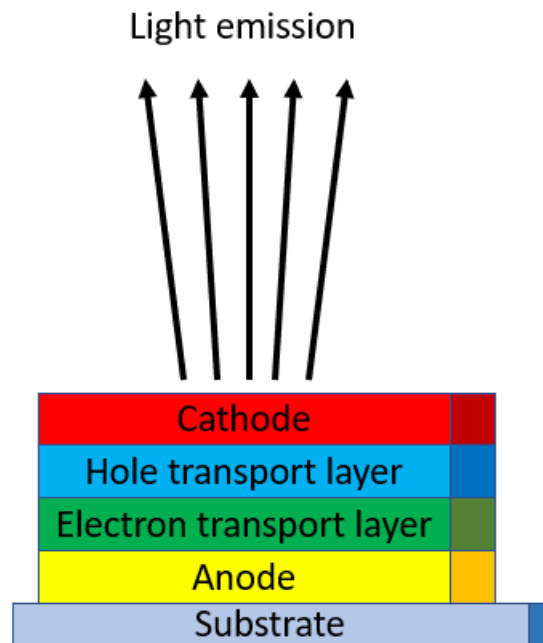
Figure 2: Structure of an OLED

There are many advantages that OLEDs have over inorganic LEDs. OLEDs do not require a back light to operate, which makes them more energy efficient than LEDs and gives them better color contrast. Also, since there are no metals used in the generation of light, OLEDs are much more flexible than LEDs, allowing them to be used in larger displays and in more complex shapes.

However, there are also some disadvantages to OLEDs. Their lifespan is not as long as an inorganic LEDs lifespan. The manufacturing of OLEDs is also very complex, which makes manufacturing devices that use OLEDs expensive.[5]

1.4: Chromophores in OLEDs

As the development of OLEDs progressed, chromophores that use different emission pathways were used for light emission. Each emission path is more efficient than the previous method used. There have been four emission paths used in OLEDs: fluorescence, phosphorescence, triplet-triplet annihilation (TTA) and thermally activated delayed fluorescence (TADF).[6]
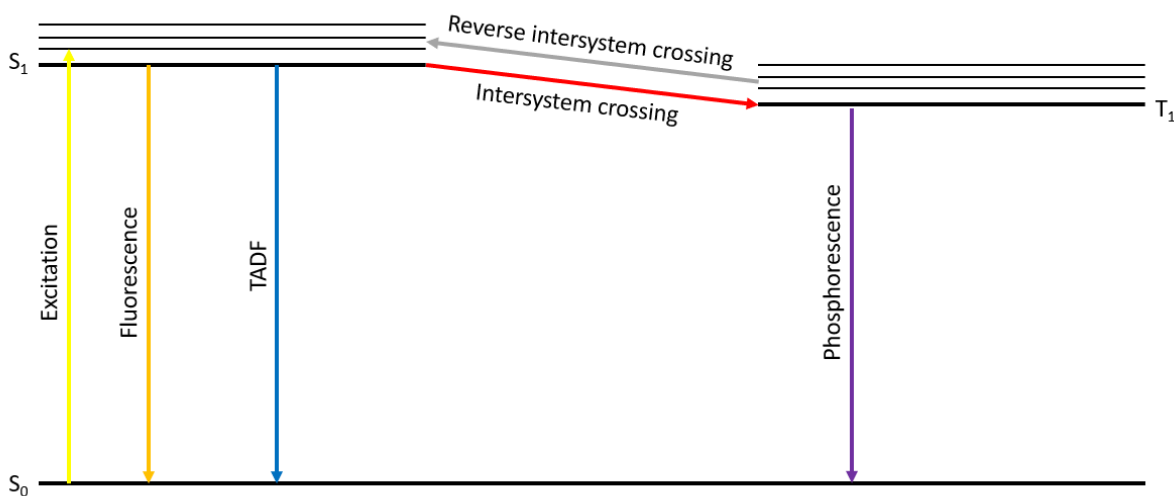
Figure 3: Jablonski energy diagram showing the emission pathways of fluorescence, phosphorescence and TADF.

The first emission path used in OLEDs was fluorescence. To generate light, fluorescence harvests the singlet state of the chromophore. When the chromophore becomes excited from S_0 to S_1, an electron in the molecule's highest occupied molecular orbital (HOMO) moves to the next higher molecular

5

orbital, the lowest unoccupied molecular orbital (LUMO). The spin of the excited electron is unchanged during this allowed singlet to singlet absorption transition. Molecules in the S_1 state release the energy absorbed by many processes, which include relaxation to the ground state with emission of light in an allowed fluorescence transition. Chromophores that use fluorescence to emit have a larger energy gap (ΔE) between the singlet state and the triplet state, which prevents crossing to the triplet state. There are two efficiencies that are measured to determine the efficiency of a chromophore: internal quantum efficiency (IQE) and external quantum efficiency (EQE). The IQE measures the efficiency of the excitation of the chromophore and tells how energy demanding the chromophore will be. EQE measures the emitted light of the chromophore, comparing the energy input against the energy that is released through the emission method the chromophore uses. Any energy that is not released as light is lost as heat. Due to only the singlet state being harvested, the theoretical IQE of fluorescence is limited to 25% when excited using an electric current. Due to this low IQE, more efficient emission pathways were explored.[6]

Phosphorescence generates light by having the chromophore go from an excited triplet state to the ground singlet state. Excitation of the T_1 triplet state may occur directly by electric current excitation or by intersystem crossing (ISC). The ISC path is spin forbidden, but the presence of heavy transition metals, such as platinum or palladium, allows electrons to change their spin in the transition from the excited singlet state to the triplet state. In a phosphorescence system, molecules excited to the S_1 state may relax partially using fluorescence;

6

however, most of the excited electrons will change their spin to an excited triplet state (T_1) via intersystem crossing. Phosphorescent systems also have a large ΔE between S_1 and T_1, which prevents intersystem crossing from occurring in a fluorescent system, but the heavy transition metal allows electrons to change their spins to T_1. Once the T_1 state is populated, the chromophore has to relax back to S_0 and it has two paths it can use: undergo the spin forbidden emission path back to the ground state or lose the energy as heat. The spin forbidden path emission is enhanced in a phosphorescence system due to the heavy transition metal assisting in spin coupling. A system that uses phosphorescence excited by an electrical current has an IQE of 100% and will emit light for a longer amount of time than fluorescence once excitation has ceased. The longer emission time in a phosphorescence system is due to the bottleneck of electrons in the triplet state that do not want to take the spin forbidden path to the ground state.[6] However, due to the rarity of the heavy transition metals used, phosphorescent chromophores are expensive, causing cheaper options to be pursued.

Triplet-triplet annihilation (TTA) is the first delayed fluorescence method that was used in OLEDs. To generate light, TTA uses the impact of two molecules. The TTA system is composed of two parts: the sensitizer species and the annihilator species. The sensitizer is typically composed of a platinum or palladium porphyrin and operates similar to a phosphorescent system. In a TTA system, the sensitizer becomes excited and will move to S_1. Once there, intersystem crossing populates T_1, which is allowed due to a heavy metal being present. Once in the triplet state, the annihilator species becomes excited via

triplet energy transfer, which is similar to intersystem crossing, but takes place between two triplet states rather than a singlet and triplet state. Once the annihilator species is excited, two annihilators collide, which allows the chromophore to relax to S_0 and release light. Fluorescence still occurs in a TTA system, but the light generated by the annihilators is much more intense. When added with the base 25% IQE that fluorescence provides, a TTA system that is excited by an electrical current has the potential for an IQE of 62.5%.[7]
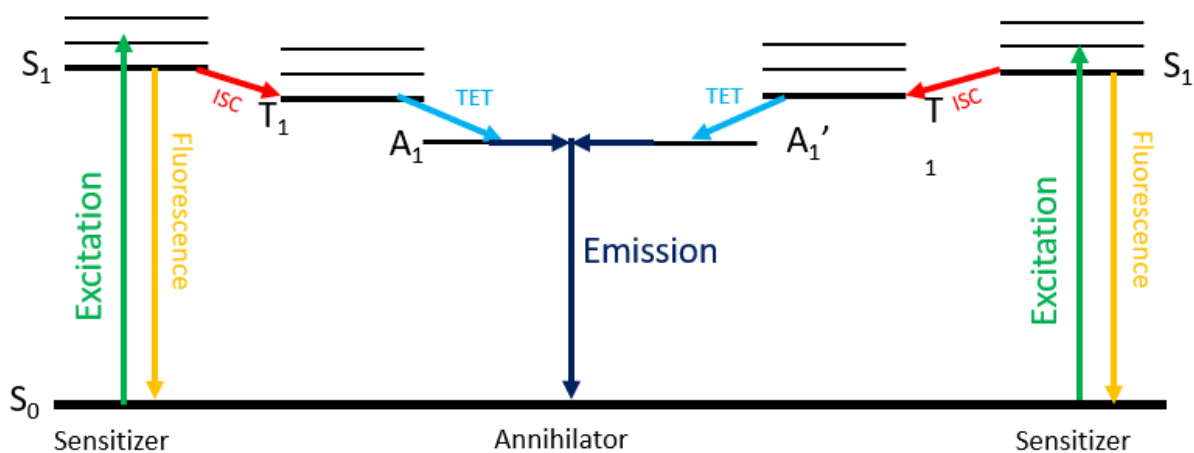
Figure 4: Jablonski energy diagram showing the emission path of triplet-triplet annihilation

Recently, a second delayed fluorescence method has begun to be used in OLEDs. Thermally activated delayed fluorescence (TADF) systems harvest both the singlet state and the triplet state. In a TADF system, molecules excited to S_1 mirror a normal fluorescence system at the start and some undergo fluorescence right away. In a TADF system however, electrons will change their spin to T_1 via

intersystem crossing. This is possible without a heavy metal due to a TADF system having a small ΔE between S_1 and T_1. Since the path from the triplet state to the ground state is forbidden and there is no heavy metal to promote it, fluorescence being a kinetically favored emission path over phosphorescence and the small ΔE between energy states, the molecules that switched to the triplet state will cross back to the singlet state. From there, they undergo fluorescence to the ground state, releasing light. Since TADF systems harvest the electrons that crossed to T_1, along with the electrons that did not, a TADF system excited by an electric current can have a theoretical IQE of over 99%.[6]

1.5: TADF Background

TADF systems rely on the small energy gap between the S_1 and T_1. This energy gap (ΔE_{S-T}) determines the efficiency of the system. The bandgap measures the energy difference between the highest occupied molecular orbital (HOMO) and the lowest unoccupied molecular orbital (LUMO). A larger bandgap causes the generated light to be blue, and a smaller bandgap causes generated light to be red.

TADF systems are composed of two parts: an electron rich donor group (F**igure 6**) and an electron poor acceptor group (**Figure 5**). The donor group contains the HOMO, and the acceptor group contains the LUMO. Through changing the groups, the bandgap is able to be tuned. By using large, bulky groups that disrupt the planarity of the molecules, you can ensure that the energy

gap between S_1 and T_1 is small enough that reverse intersystem crossing is efficient, making TADF possible.[6]
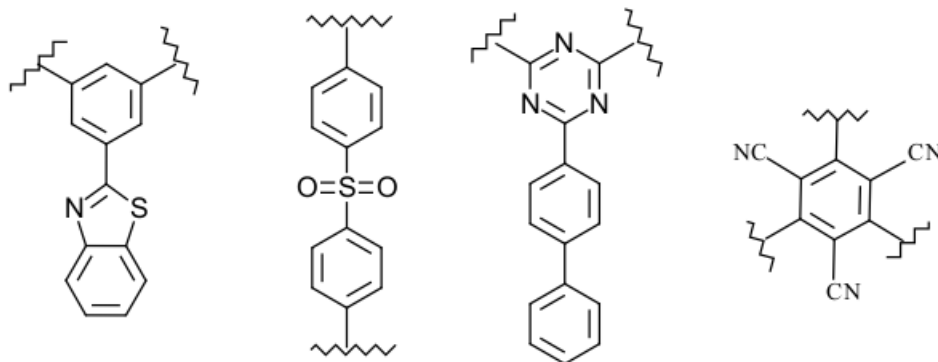
Figure 5: Examples of TADF acceptor groups

By changing the donor and acceptor group of a TADF system, the band gap is tunable by using large, bulky groups that force the molecule out of planarity. This separates the HOMO and the LUMO and provides a small ΔE_{S-T} that allows TADF to occur.
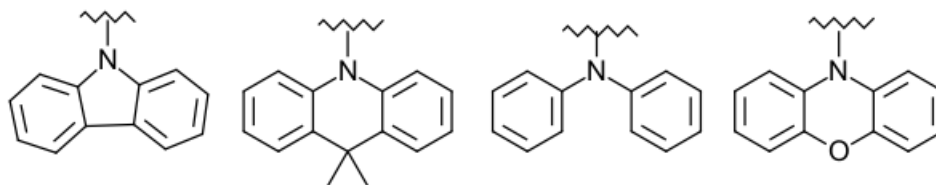
Figure 6: Examples of TADF donor groups

A study done in 2012 by Adachi *et al.* demonstrated the design of an efficient, blue emitting chromophore. The compound, 2,4-bis{3-(9 H-carbazol-9-yl)-9 H-carbazol-9-yl}-6-phenyl-1,3,5-triazine (**Figure 7**), is composed of a

triazene derivative that is the acceptor ground and bicarbazole, which is the donor group. The light that the compound emitted had a wavelength of 435 nm, placing the color of the emitted light in the blue region of the visible spectrum. This compound had an external quantum efficiency (EQE) of 11 $\pm$ 1%, showing how TADF systems are much more efficient than a traditional fluorescence system and are on par with phosphorescent systems.[8]
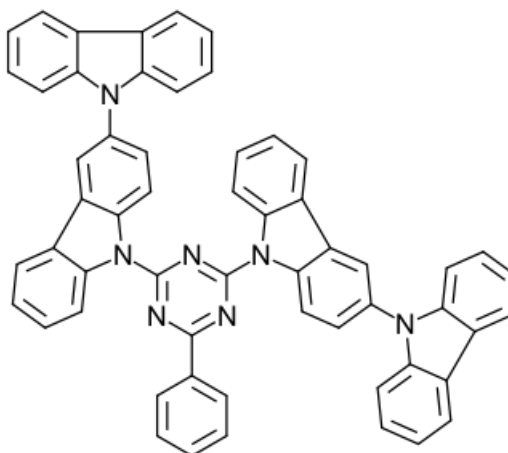
Figure 7: Blue emitting TADF compound by the Adachi research group

In 2016, Lee and Lee published their work with a blue emitting TADF chromophore had an EQE of nearly 20%. The compound was designed based off of work done in the past by the Adachi group, with 9,9-dimethyl-9H-thioxanthene 10,10-dioxide acting as the acceptor group and 9,9'-dimethylacridine. The efficiency of this compound was due to a slight overlap in the HOMO and the LUMO, which allows reverse intersystem crossing to happen easily.[9]
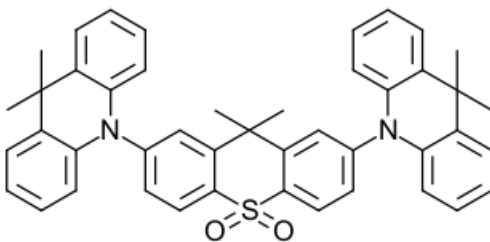
Figure 8: TADF emitter made by Lee and Lee

This TADF compound is unique in that it has a very narrow emission

range. Previous TADF compounds had a broad emission range. For example,

the Adachi compound has an emission range that is greater than 65 nm at half

peak high. The compound developed by Lee and Lee has an emission range of

61 nm at half peak height, which improves the color purity of the emitted light.

The narrower emission range in this compound comes from the restricted

molecular movement caused by bridging between the diphenyl sulfone acceptor

group.

1.6: Polymers and OLEDs

While TADF compounds are breakthrough and are making massive

strides to become the primary emission method for OLEDs, they have their

drawbacks. TADF compounds on their own are not well suited for used in

OLEDs, as they crystallize very easily, making them very difficult to process for

use in displays. The most common form of processing TADF compounds for

devices is vacuum deposition, which is incredibly expensive and limits the size of

the devices. Due to these limitations, these devices are only suitable for use in smaller displays, such as in smartphones or other handheld devices.[10]

To combat the limitations observed with just using TADF compounds in displays, work with combining TADF compounds with polymers began. Polymers are much easier to process, with methods such as spin casting or inkjet printing being used. Through the combination with polymers for use in an OLED, TADF emitters become better suited for use in larger displays and become more flexible. Work with polymers that undergo electroluminescence has occurred since the 1990s, when fluorescence was observed in poly(p-phenylenevinylene), a conjugated system. Since work began with electroluminescent polymers, both non-conjugated and conjugated polymers that use the various emission pathways available have been studied and used. However, due to the high EQE that is offered by TADF, focus has shifted to polymers that utilize it.[11]

A polymer that utilizes TADF must be structured similar to how a small molecule TADF emitter is structured. There must be a small ΔE_{S-T} for efficient reverse intersystem crossing to occur. However, achieving an efficient, strong emission in a conjugated system is difficult.

As shown in **Figure 9**, there are four main designs for a TADF polymer: 1) alternating between the donor groups and the acceptor groups as the backbone of the polymer, 2) alternating a TADF emitter with a second backbone unit, 3) a polymer backbone composed of donor groups with the acceptor groups attached as side-chains and 4) a polymer composed of a backbone unit with the TADF emitter attached as a pendant group. The approach used in this project is a mix

13

of the second and fourth designs, where part of the TADF emitter is incorporated

into the polymer backbone and the donor group is attached as a pendant

group.[12]
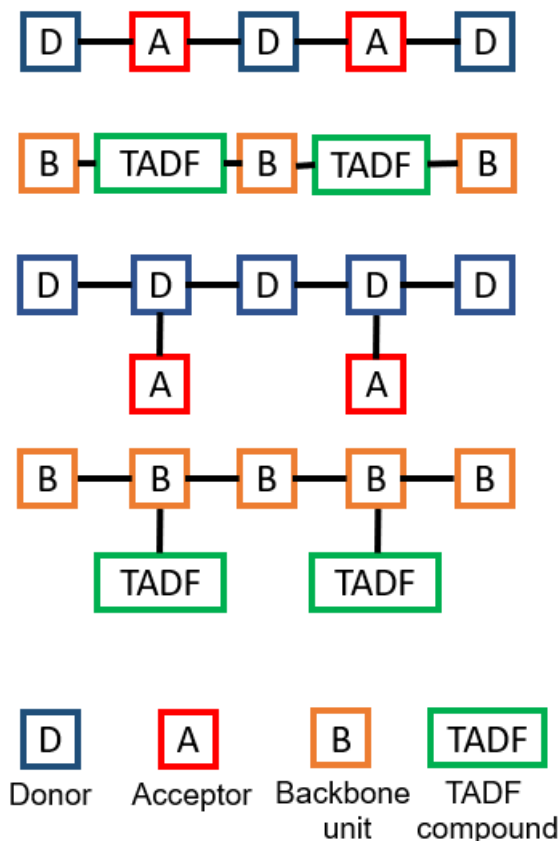
Figure 9: The four primary TADF polymer designs

An example of the second design used by a TADF polymer comes from a

study by Nikolaenko *et al.* In this study, a TADF polymer using N,N′-bis(4-

hexylphenyl)- N,N′-bis(4-(4,4,5,5-tetramethyl-1,3,2-dioxaborolan-2-

yl)phenyl)benzene1,4-diamine was used as the donor group, 2,4-bis(4-

bromophenyl)- 6-(4-dodecylphenyl)-1,3,5-triazine as the acceptor group and 1,4-

bis(4-(4,4,5,5-tetramethyl-1,3,2-dioxaborolan-2-yl)phenyl) butane as the

backbone unit. These compounds were used in a ratio of 50% acceptor group, 45% backbone unit and 5% donor group. This TADF compound emitted light in the green region with coordinates in the Commission Internationale de L'Eclairage (CIE) of 0.32, 0.58. When used in an OLED, the device had an EQE of 10%.[13]
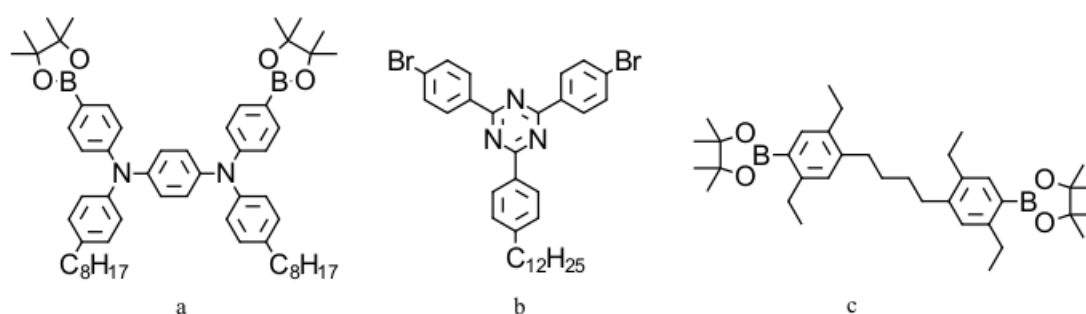
Figure 10: Structures of the donor group (a), the acceptor group (b), and the backbone unit (c) used by the Nikolaenko group
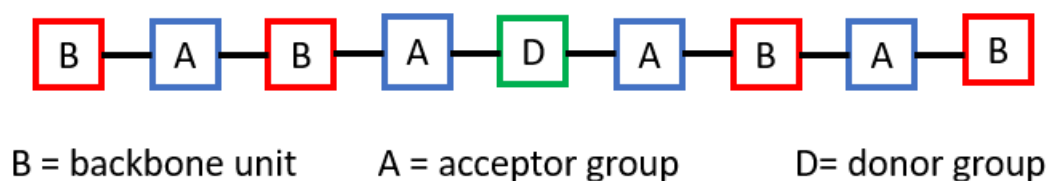
Figure 11: Polymer design used by the Nikolaenko group

An example of the fourth TADF polymer design comes from a study done by Nobuyasu *et al.* In the study, a TADF polymer was made from phenothiazine

as the donor group, with dibenzothiophene-S,S-dioxide as the acceptor group. There were two backbone compounds used as the polymer, styrene and dibenzothiophene. The copolymers were made with a composition of 63% of the donor group and 37% acceptor group. The polymer emitted light in the green range with a wavelength of 540 nm.[14]
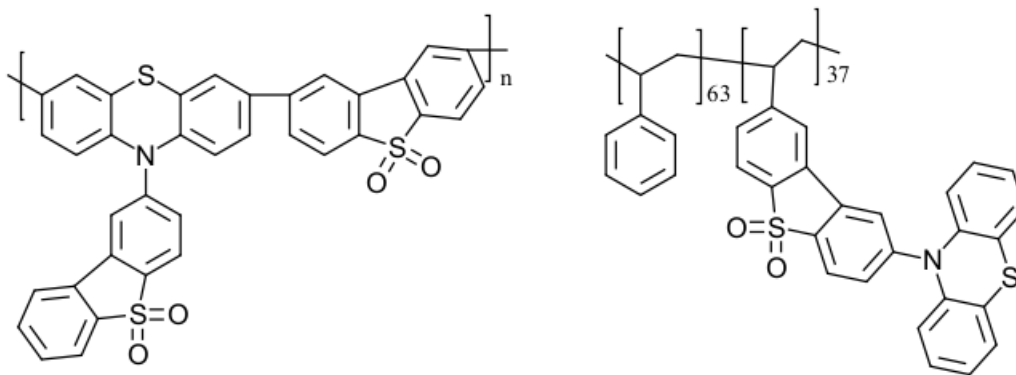
Figure 12: Repeat units of TADF polymers used by Nobuyasu

1.7: Poly(arylene ether)s

For TADF polymers, the material that the backbone is made of determines how well the device will work. Backbone units that promote long term stability of the chromophore are desired. Thermoplastics are used as backbones units frequently, due to their easy processing methods, and their ability to be constantly molded and remolded to different shapes and retain their physical properties, as well as offering the desired physical properties.[15] A backbone unit that has become more and more commonly used is poly(arylene ether)s. This class of thermoplastics have a structure of aromatic rings that are connected by

ether bonds. The structure of poly(arylene ether)s are rigid and have a high electron density due to the aromatic rings. The rigidity and electron density give these polymers very desirable thermal and mechanical properties. By using PAEs as the backbone unit, there is the potential to increase the lifespan of the OLED by adding thermal stability to the TADF emitter. There is also the potential to increase the EQE of the emitter by preventing self-aggregation and self-quenching.[16]

1.8: Nucleophilic Aromatic Substitution (NAS)

Small molecule TADF emitters can easily be designed to resemble monomer units that can be used in nucleophilic aromatic substitution (NAS) polymerization reactions. This allows them to be incorporated into a PAE backbone with relative ease. The small molecule TADF emitters act as dopants in the backbone polymer, forming a guest-host system that can act as the light emitting layer in an OLED. For a TADF compound to be incorporated into a polymer, there must be a designed site for the polymerization to occur. These sites are typically halide leaving groups, such as fluoride or chloride. In this mechanism, the *ipso* carbon becomes the electrophile that will be attacked by the nucleophile. Once the nucleophile attacks, the aromaticity will be broken, and a resonance stabilized intermediate is formed. Aromaticity is restored when the leaving group leaves the ring.[17]
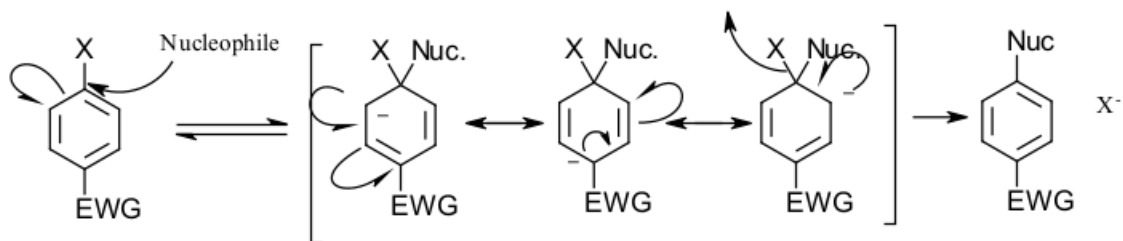
Scheme 1: General mechanism of NAS

There are two main strategies for adding TADF emitters into the backbone of a polymer: functionalizing the TADF unit before it is incorporated into the polymer and functionalizing the TADF unit after it has been incorporated into the polymer. In pre-functionalization, the donor group is added to the acceptor to complete the emitter before the polymerization reaction takes place. In post-functionalization, a leaving group must survive the polymerization reaction. Once the polymerization is complete, the surviving leaving group is displaced by the donor group.
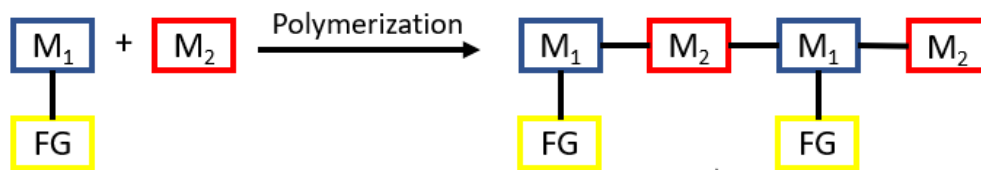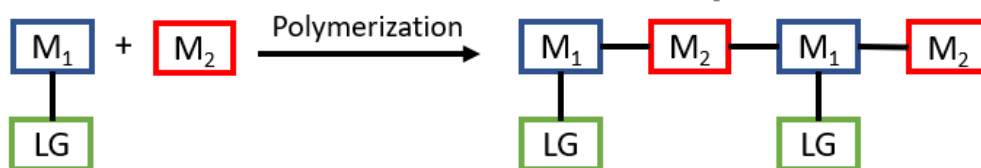
Figure 13: Both TADF addition strategies

1.9: Previous work

Group work on the inclusion of blue emitting TADF compounds into PAE backbones began with Picker's[18] project that utilized iodinated 3,5-difluorodiphenylsulfone (3,5-DFDPS-I). Picker initially attempted to use post-functionalization but was unsuccessful. Instead, pre-functionalization was used. To replace the iodine, a copper catalyzed carbon-nitrogen coupling reaction was used to add carbazole and other donor groups. The pre-functionalization rout was successful. From there, a polymerization reaction was done using the completed TADF monomer, 4,4'- difluorodiphenylsulfone (DPS), and bisphenol A (BPA). Several varieties of copolymers were made. Each copolymer made had

high thermal stabilities. Films cast of the polymers had a broad emission from 370 nm to 600 nm with peak emission at 430 nm.
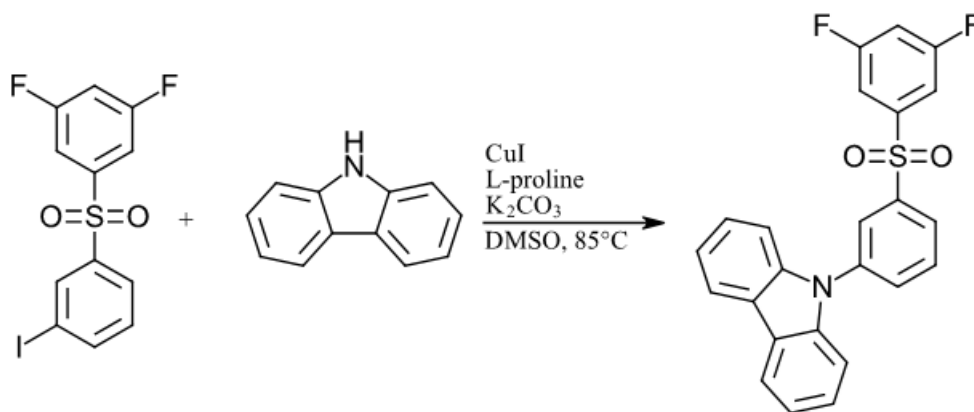
Scheme 2: Synthesis of Picker's 3,5-DFDPS-CBZ TADF chromophore
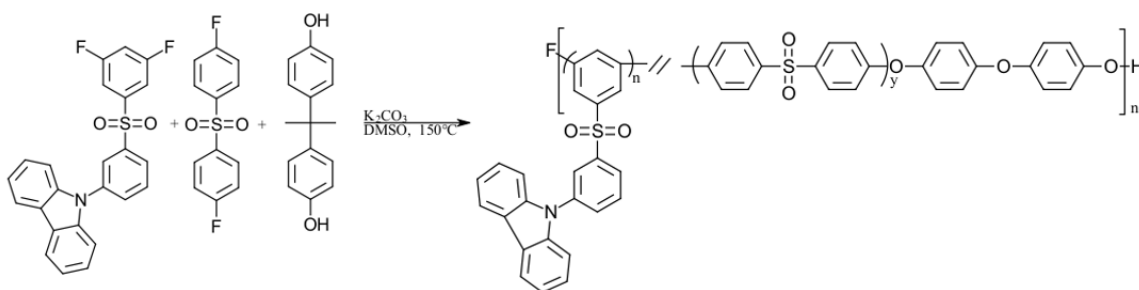
Scheme 3: Picker's incorporation of the 3,5-DFDPS-CBZ TADF chromophore into a PAE system

Continuing work in TADF polymers, Kemboi[19] began a project involving benzoxazole and benzothiazole based chromophores. These compounds were functionalized using carbazole and indole donor groups. Examples of monomers that were synthesized are benzoxazole-carbazole (BOX-CBZ), benzoxazole-

indole (BOX-IND) and benzothiazole-carbazole (BTZ-CBZ). When dissolved in

THF, these compounds were excited with both short wave (256 nm) and long

wave (365 nm). This resulted in a broad emission of 403 nm to 473 nm, with a

peak at 460 nm. The monomers made were polymerized via a NAS

polycondensation reaction, using 4,4'-difluorotriphenylphosphine oxide (dFTPPO)

and 4,4'-biphenol as other monomers. Thermal analysis of the polymers showed

that the copolymers had sufficient rigidity for use in OLEDs and a T_g range of

241°C to 243°C. Films were cast of the copolymers as well. Films cast using

benzoxazole copolymers emitted light at 430 nm and films cast using

benzothiazole copolymers emitted light at 451 nm, true blue.
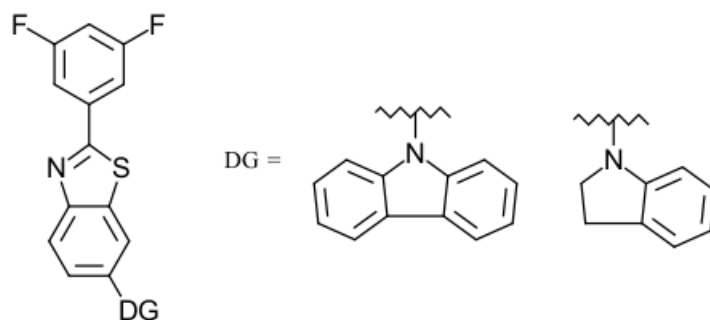
Figure 14: Kemboi's benzothiazole based blue emitting TADF chromophore
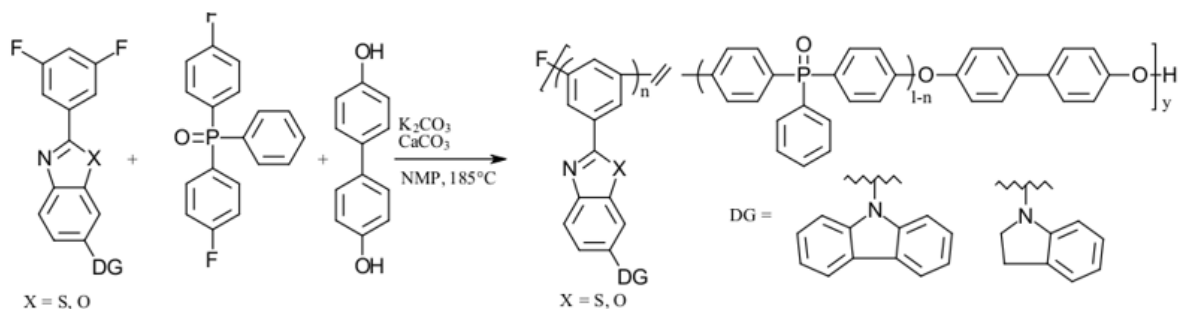
Further exploring benzoxazole polymers, Slaybaugh[20] synthesized
different regio-isomers. A 2,4-difluoro derivative was synthesized and
functionalized using carbazole. When dissolved in THF and excited under long
wave UV light, a peak emission of 430 nm was observed. When compared to the
3,5-difluoro derivative, a 30 nm blue shift was observed. This benzoxazole
derivative was then polymerized with two different backbone compounds:
DPS/BPA and dFTPPO/4,4'-dihydroxydiphenyl ether (DPE). Thermal analysis of
these copolymers revealed a T_g range of 182°C to 206°C. Films cast from the
copolymers had emissions of deep blue light, with a peak emission at 416 nm.
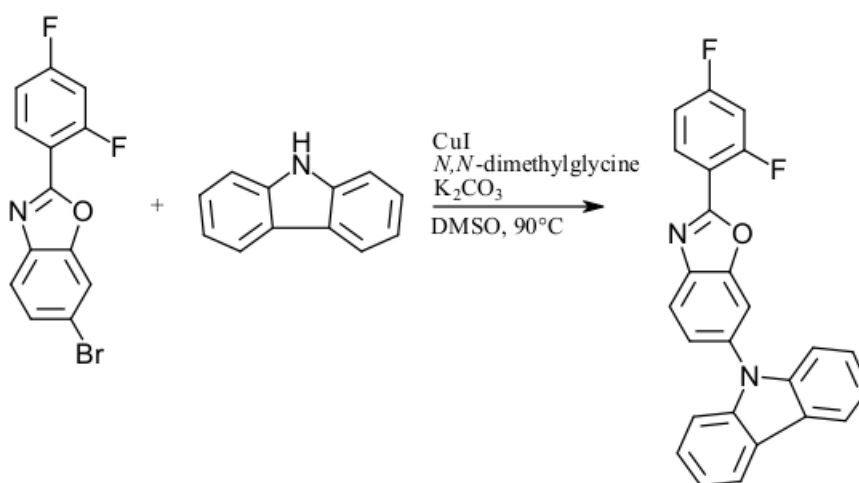
Scheme 5: Slaybaugh's synthesis of 2,4-diF-BOX-CBZ
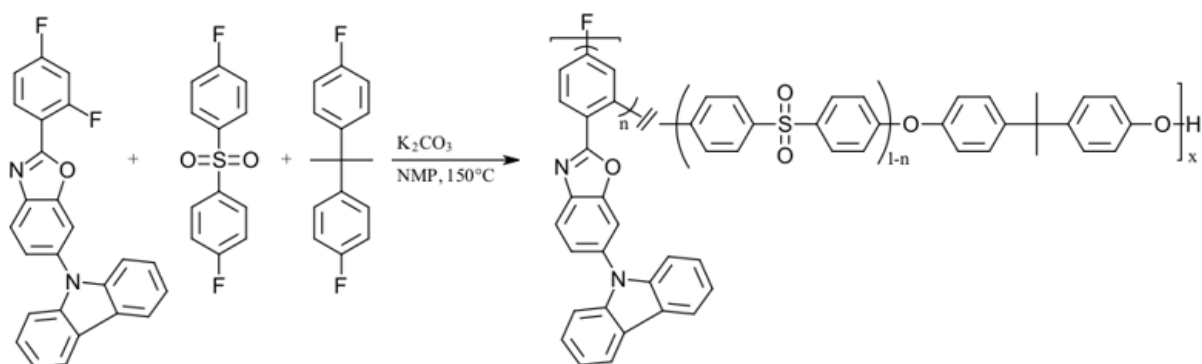
Scheme 6: Slaybaugh's polymerization of 2,4-diF-BOX-CBZ with bisphenol A

Most recently, Fetters[16] explored incorporating benzophenone based TADF chromophores into two different polymer backbones: bis-(4-fluorophenyl) sulfone/DPE and triphenylphosphine oxide/DPE. Copolymers made with the bis-(4-fluorophenyl) sulfone/DPE system had a T_g range of 180°C to 183°C and emitted light in the UV range, with a peak emission at 465 nm. Copolymers made of the triphenylphosphine oxide/DPE system had a T_g range of 181°C to 190°C and emitted light in the blue region, with a peak emission at 455 nm.
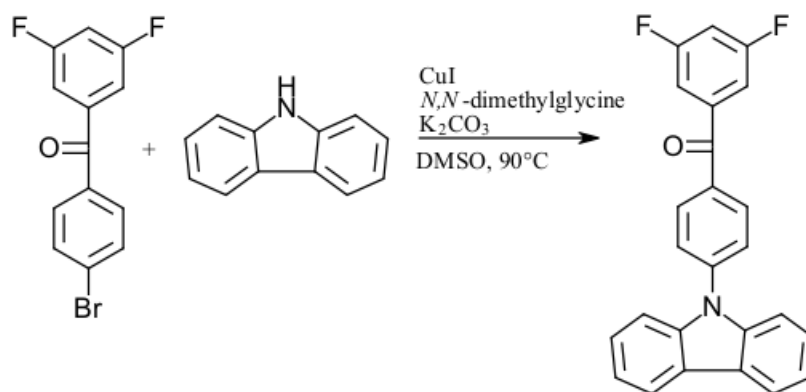
Scheme 7: Fetter's benzophenone TADF chromophore synthesis
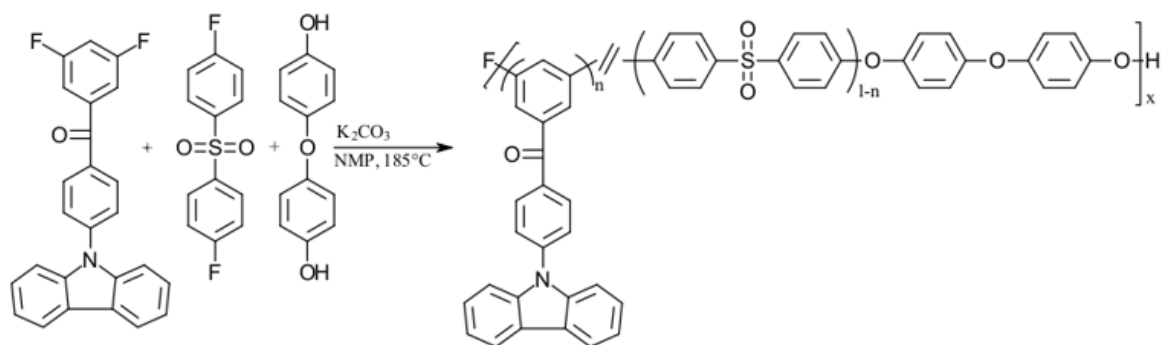
.**Scheme 8:** Fetter's 3,5-DFK-CBZ DPS/DPE polymer synthesis

Groups outside of the Fossum research group have been doing work involving PAE backbones with TADF chromophores has been done. Yang *et al.* shared work with red-emitting TADF polymers in 2018. The TADF emitter, 2-(N-(4- octyloxyphenyl)diphenylamino)-4'-anthraquinone was embedded in poly(fluorene-co-3,3'-dimethyl diphenyl ether). This polymer had a relatively low T_g range from 86°C to 88°C and emitted red light with a peak emission of 606 nm. The EQE of the TADF polymer was found to be 5.6%. Several copolymers were made using this combination of TADF emitter and backbone polymer at different ratios of the emitter. As more TADF emitter was incorporated into the polymer, the emitted light became red-shifted.[16]
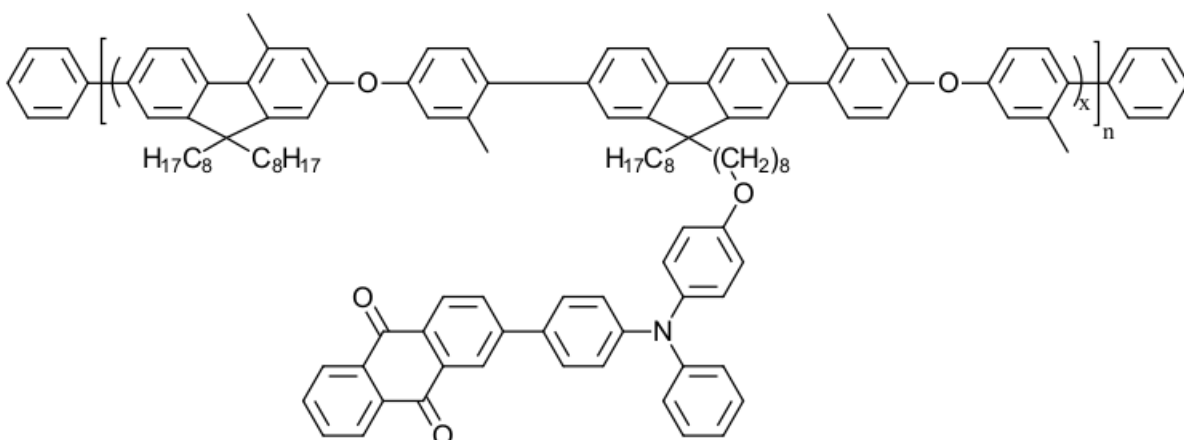
Figure 15: Red emitting TADF polymer made by the Yang research group

1.10: Current Work

The primary goal of this project was to increase the efficiency a blue-emitting, benzothiazole based TADF chromophore through covalent bonding to different PAE host polymers. The chromophore selected to be covalently attached to the polymers was 3,5-difluorobenzothiazole-carbazole (3,5-diF-BTZ-CBZ). The host polymer must promote a small energy gap between the singlet state and the triplet state to assist in intersystem and reverse intersystem crossing, increasing the EQE of the TADF chromophore. The polymers developed are intended to replace either the hole-transport layer or the electron-transport layer of an OLED. The TADF chromophore was incorporated at different weight percentages and films were cast of the resulting copolymers.
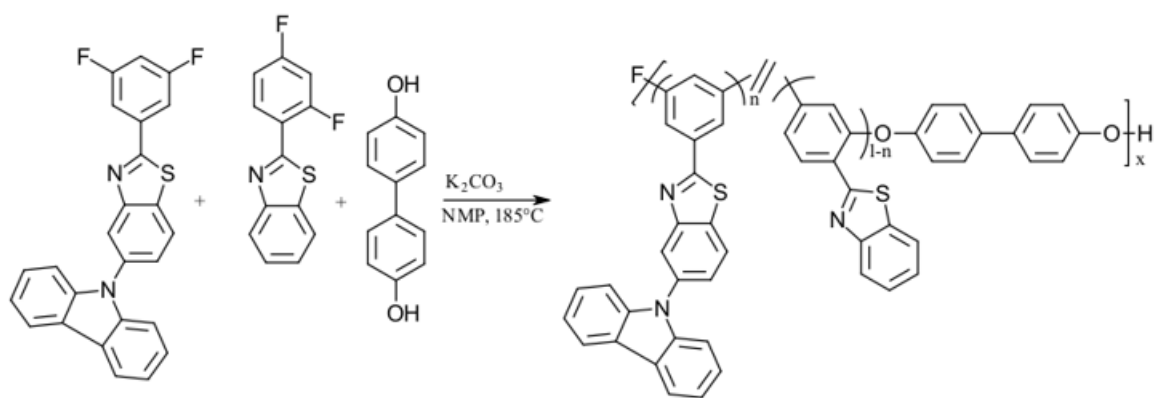
Scheme 9: Polymer synthesis incorporating 3,5-diF-BTZ-CBZ into a PAE system

2. Experimental Methods

2.1: Materials The compounds 3,5-dilfluorobenzoic acid, 2,4-difluorobenzoic acid, sodium bicarbonate, hexanes, isopropanol and *N*-iodosuccinimide (NIS) were purchased from Oakwood chemicals and were used as received. The compounds acetonitrile, $CDCl_3$, carbazole, copper (I) iodide (CuI), *N,N*-dimethylglycine, potassium carbonate and 2-aminothiophenol were purchased from Sigma-Aldrich. Acetonitrile, $CDCl_3$, carbazole, *N,N*-dimethylglycine, potassium carbonate and 2-aminothiophenol were used as received. Copper (I) iodide was activated using a Soxhlet extractor using tetrahydrofuran (THF). The compounds magnesium sulfate, sodium bisulfite, dimethyl sulfoxide, and tetrahydrofuran (THF) were all purchased from Fischer Scientific and used as received. The compounds 4,4'-dihydroxydiphenyl ether, 4,4'-biphenol and 9,9-dihydroxydimethyl acridine were purchased from TCI and used as received. Ethanol was purchased from Decon Laboratories and was used as received. Chloroform was purchased from EDM Millipore Corp and was used as received. Sulfuric acid was purchased from Acros Organics and was used as received.

2.2: Instrumentation

A Bruker AVANCE 300 MHz Nuclear Magnetic Resonance (NMR) spectrometer was used to acquire ^1H spectra, operating at 300 MHz. All samples were dissolved in $CDCl_3$. A Hewlett-Packard (HP) 6890 series GC, paired with a HP 5973 mass selective detector/quadrupole was used to perform GC/MS analysis. Thermogravimetric analysis (TGA) and differential scanning calorimetry (DSC) were performed on TA instruments TGA Q500 and DSC Q200 under nitrogen heating at 10°C per minute. Melting points were observed on an Electrothermal Melting Point Apparatus and are uncorrected. UV/Vis absorbance spectra were acquired on an Agilent Cary 60 UV/Vis Spectrometer. Fluorescence emission spectra were gathered on a Horiba/Jobin Yvon Sygnature monochromator with an excitation wavelength of 365 nm.

2.3: Synthesis of 2-(3,5-difluorophenyl)-benzathiozole

To a 250mL round bottomed flask (RBF) equipped with a condenser, gas inlet and a magnetic stir bar, were added polyphosphoric acid (52 g), 3,5-difluorobenzoic acid (5 g, 31.65 mmol) and 4.75 mL of 2-aminothiophenol (5.7 g, 45.5 mmol). The reaction mixture was then heated at 90°C until the 3,5-difluorobenzoic acid stopped subliming, then the temperature was increased to 150°C and stirred for 24 hours, at which point it was allowed to cool to room temperature and was added dropwise to 6 L of vigorously stirred water. The resulting solids were isolated via vacuum filtration. The crude product was taken up in excess ethyl acetate and transferred to a 500 mL separatory funnel. The organic layer was washed twice each of brine, 5% sodium bicarbonate solution

and water. The organic layer was collected and dried over magnesium sulfate, filtered and the ethyl acetate was then removed using a rotary evaporator. The resulting solids were taken up in chloroform and decolored using activated carbon, filtered and the chloroform was removed using a rotary evaporator. The resulting solids were recrystallized from 100mL of ethanol and isolated via vacuum filtration to afford 4.36g (55.8%) of the desired product as a pink/purple solid. The melting point was determined to be 104° to 106°C

2.4: Synthesis of 2-(3,5-difluorophenyl)-iodo-benzothiazole

To a 25mL RBF equipped with a condenser, gas inlet and a magnetic stir bar, were added 2-(3,5-difluorophenyl)-benzathiozole (0.502 g, 2.03 mmol) and 2mL of concentrated sulfuric acid. To a separate beaker, *N*-idodosuccinimide (0.313 g, 1.340 mmol) was dissolved in 3mL of concentrated sulfuric acid. The two mixtures were then combined dropwise in the RBF. The reaction mixture was stirred at room temperature under nitrogen for 24 hours, at which point GC/MS analysis of an aliquot precipitated from water indicated an 62% conversion rate. The reaction mixture was allowed to cool to room temperature and was added dropwise to 300 mL of vigorously stirred water. The resulting solids were isolated via vacuum filtration, then recrystallized from a mixture of one part chloroform, one part toluene and eight parts ethanol. GC/MS analysis showed a ratio of 88% mono-substituted product to 11% di-substituted product. Further recrystallization attempts did not reduce the ratio. The resulting solids were isolated via vacuum filtration, affording 0.120 g of the desired product. The melting point was found to be 117° to 122°C.

2.5: Synthesis of 2-(3,5-difluorophenyl)-benzothiazole-carbazole chromophore

To a 5mL three neck RBF equipped with a condenser, gas inlet and a magnetic stir bar, were added carbazole (1.01g, 6.04 mmol), 2-(3,5-difluorophenyl)-iodo-benzothiazole (0.75 g, 2.01 mmol), copper (I) iodide (0.038 g, 0.20 mmol), N,N-dimethylglycine (0.044 g, 0.43 mmol), potassium carbonate (0.863 g, 6.24 mmol) and 6mL of DMSO. The reaction mixture was heated to 80°C and stirred for 24 hours, at which point GC/MS analysis of an aliquot precipitated from water indicated a conversion of 96%. The reaction was then allowed to cool to room temperature and added dropwise to 1L of vigorously stirred water. The resulting solids were isolated via vacuum filtration and taken up in 100mL of chloroform and added to a 250mL separatory funnel and washed with 200mL of a brine solution. The organic layer was collected, dried over magnesium sulfate and the chloroform was removed using a rotary evaporator. The resulting solids were then recrystallized from a solution of 8:2 chloroform and ethanol and isolated via vacuum filtration to afford 0.303 g (36.4%) of the desired product. The melting point was determined to be 175°C to 177°C. ^{1}H NMR data was acquired by Abraham Kemboi.

^{1}H NMR (CDCl$_3$; δ): 7.01 (tt, $^3J_{H-F}$ =8.6, $^4J_{H-H}$ =2.3, 1H), 7.35 (ddd, $^3J_{H-H}$ =7.9, $^3J_{H-H}$ =4.6, $^4J_{H-H}$ =3.4, 2H), 7.47-7.45 (m, 4H), 7.71-7.68 (m, 2H), 7.75 (dd, $^3J_{H-H}$ =8.7, $^4J_{H-H}$ =2.1, 1H), 8.12 (dd, $^4J_{H-H}$ =2.1, $^5J_{H-H}$ =0.5, 1H), 8.19 (M, 2H), 8.31 (dd, $^3J_{H-H}$ = 8.7, $^5J_{H-H}$ =0.5, 1H)

2.6: Synthesis of 2-(2,4-difluorophenyl)-benzothiazole

To a 250mL RBF equipped with a condenser, gas inlet and a magnetic stir bar, were added polyphosphoric acid (50.5 g), 2,4-difluorobenzoic acid (5.05 g, 20.5 mmol) and 4.75mL of 2-diaminothiophenol (5.7 g, 45.5 mmol). This reaction mixture was then heated at 90°C until the 2,4-difluorobenzoic acid stopped subliming, at which point the temperature was increased to 150°C and stirred for 24 hours, at which point it was allowed to cool to room temperature and was added dropwise to 3L of vigorously stirred water. The resulting solids were isolated via vacuum filtration. The crude product was taken up in excess ethyl acetate and transferred to a 500 mL separatory funnel. The organic layer was washed with two washes of brine and two washes of a 5% sodium bicarbonate solution. The organic layer was collected and then dried over magnesium sulfate, filtered and the ethyl acetate was then removed using a rotary evaporator. The resulting solids was then taken up in chloroform and decolored using activated carbon, filter and the chloroform was removed using a rotary evaporator. The resulting solids were recrystallized 100mL of ethanol and isolated via vacuum filtration to afford 3.25 g (41.1%) of the desired product. The melting point was determined to be 104° to 106°C.

^{1}H NMR (CDCl$_3$; δ): 7.03 (m, 2H), 7.42 (td, $^3J_{H-H}$ =7.76, $^3J_{H-H}$ =7.02, 1H), 7.52 (td, $^3J_{H-H}$ =7.76, $^3J_{H-H}$ =7.76, 1H), 7.94 (d, $^3J_{H-H}$ =8.13, 1H), 8.10 (d, $^3J_{H-H}$ =8.12, 1H), 8.44 (m, 1H)

2.7: Synthesis of 2-(2,4-diflurophenyl)-benzothiazole-dihydroxydiphenyl ether polymer

To an oven dried 5 mL RBF, equipped with a condenser, gas inlet, and a magnetic stir bar, were added 2-(2,4-difluorophenyl)-benzothiazole (0.210 g, 0.85 mmol), potassium carbonate (0.36 mg, 2.58 mmol), dihydroxydiphenyl ether (0.17 mg, 0.85 mmol) and 1.26 mL of NMP. This reaction mixture was then heated at 160°C and stirred for 60 hours, at which point it was cooled to room temperature and added dropwise to 300 mL of vigorously stirred water. The resulting solids were isolated via vacuum filtration to afford 0.25 g of the crude product as a solid. The recovered solids were then taken up in minimal THF and then precipitated from 200 mL of a 1:1 hexanes and IPA mixture. The resulting solids were isolated via vacuum filtration to afford 73.5 mg (21.0%) of the desired product as a solid.

^{1}H NMR (CDCl$_3$; δ): 6.57 (s, 1H), 6.76 (d, $^3J_{H-H}$ =9.01, 1H), 6.96 (d, $^3J_{H-H}$ =5.38, 1H), 7.05 (s, 1H), 7.32 (s, 1H), 7.43 (s, 1H), 7.82 (d, $^3J_{H-H}$ =7.95, 1H), 8.03 (d $^3J_{H-H}$ =7.95, 1H), 8.5 (d, $^3J_{H-H}$ =9.17, 1H)

2.8: Synthesis of 2-(2,4-difluorophenyl)-benzothiazole-biphenol polymer

To an oven dried 5 mL RBF, 2-(2,4-difluorophenyl)-benzothiazole (0.20 g, 0.82 mmol) was added along with potassium carbonate (0.34 g, 2.46 mmol), biphenol (0.15 g, 0.83 mmol) and 1.26 mL of NMP. This solution was then heated at 160°C and stirred for 60 hours. The solution was cool to room temperature and

was added dropwise to 300 mL of vigorously stirred water. This was then filtered via vacuum filtration to afford 0.32 g of polymer were recovered. The polymer was then heated in minimal toluene and filtered. The recovered solids were then taken up in minimal chloroform and precipitated in 100 mL of a 50:50 mixture of hexanes and isopropanol. The resulting solids were isolated via vacuum filtration to afford 321 mg (98.64%) of the desired product.

^{1}H NMR (CDCl$_3$; δ): 6.70 (s, 1H), 6.86 (d, $^3J_{H-H}$ =7.62, 1H), 7.07 (dd, $^3J_{H-H}$ =7.03, $^3J_{H-H}$ =7.62, 1H), 7.28 (s, 1H), 7.45 (m, 2H), 7.78 (d, $^3J_{H-H}$ =8.2, 1H), 8.02 (d, $^3J_{H-H}$ =7.62, 1H), 8.54 (d, $^3J_{H-H}$ =9.37, 1H)

2.9: Synthesis of chromophore containing copolymers

To an oven dried 5 mL RBF, 2,4-difluorophenyl-benzothiazole (0.22 g, 0.91 mmol) was added along with, 2-(3,5-difluorophenyl)-benzathiozole-carbazole (0.25 mg, 0.061 mmol), potassium carbonate (0.372.1 mg, 2.6924 mmol), biphenol (0.19 g, 1.03 mmol) and 1.5 mL of NMP. This solution was then heated at 160°C and stirred for 24 hours. The solution was allowed to cool to room temperature and was added dropwise to 300 mL of vigorously stirred water. This was then filtered via vacuum filtration to afford 0.400 g of polymer. The recovered solids were then taken up in minimal chloroform and precipitated in 100 mL of a 50:50 mixture of hexanes and isopropanol. The mixture was then filtered to afford 260 mg (42.4%) of polymer.

^{1}H NMR (CDCl$_3$; δ): 6.70 (s, 1H), 6.86 (s, 1H), 7.05 (s, 1H), 7.10 (s, 1H), 7.45 (s. 7H), 7.79 (s, 1H), 8.01 (s, 1H), 8.52 (s, 1H)

33

3. Results and discussion

3.1: Synthesis of 2-(3,5-difluorophenyl)-benzothiazole, 3

The platform that will be utilized to prepare the desired blue emitting chromophore, 2-(3,5-difluorophenyl)-benzathiozole (3,5-diF-BTZ), was synthesized following the procedure previously described by Kemboi, as detailed in section **2.1**. The reaction of 3,5-difluorobenzoic acid (**1**) with 2-aminothiophenol (**2**) using polyphosphoric acid (PPA) as both the catalyst and solvent, was performed twice, each being monitored by analyzing an aliquot via GC/MS. The yields of the desired product, after work-up to afford a pink/purple solid are listed in **Table 1**. GC/MS analysis confirmed the identity of the compound, as the m/z value and fragmentation pattern matched that observed during previous work done by Kemboi[19]. Further confirmation of the structure was provided ^{1}H NMR spectroscopy. Purity was confirmed via melting point, with a melting point determined to be 104°C to 106°C, which matched the value reported by Kemboi.[19]
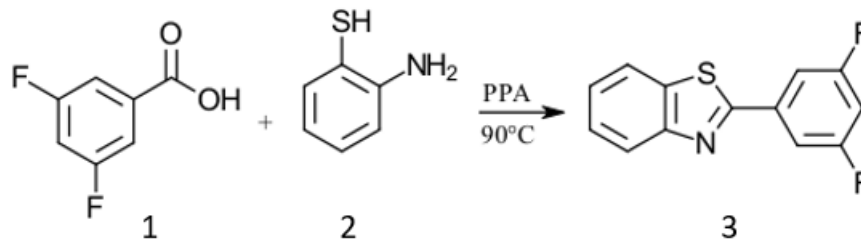
Scheme 10: Synthesis of 3,5-diF-BTZ

Synthesis	Yield	Percent yield
Run 1	1.3g	20.2%
Run 2	4.3g	55.8%

Table 1: Synthesis of 3,5-diF-BTZ and the yields of reaction

3.2: Synthesis of 2-(3,5-difluorophenyl)-iodo-benothiazole, 5

The chromophore precursor, 2-(3,5-difluorophenyl)-iodo-benzothiazole (3,5-diF-BTZ-I), was synthesized following the procedure described by Kemboi, detailed in section **2.2**. The reaction was run a total of 7 times however, the desired compound was never purified to completely remove a persistent by-product, which was identified as a di-iodinated species. Depending on the reaction conditions, each reaction had a different ratio of the desired mono-substituted product and di-substituted by-product, as determined by monitoring via GC/MS analysis. A GC/MS trace can be seen in **Figure 16**. The peak seen at 4 minutes is unreacted 3,5-diF-BTZ, the peaks seen around 6 minutes are the desired mono-iodinated product and the peaks seen around 7.75 minutes are the di-iodinated by product. The melting point confirmed the presence of the di-substituted impurity, with a broad melting point determined to be 117°C to 122°C.

The highest purity achieved through recrystallization and triturations was 3% of the di-iodinated by-product to 97% of the mono-iodinated product.
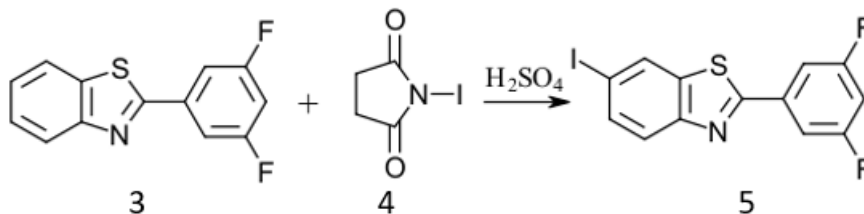
Scheme 11: Synthesis of 3,5-diF-BTZ-I
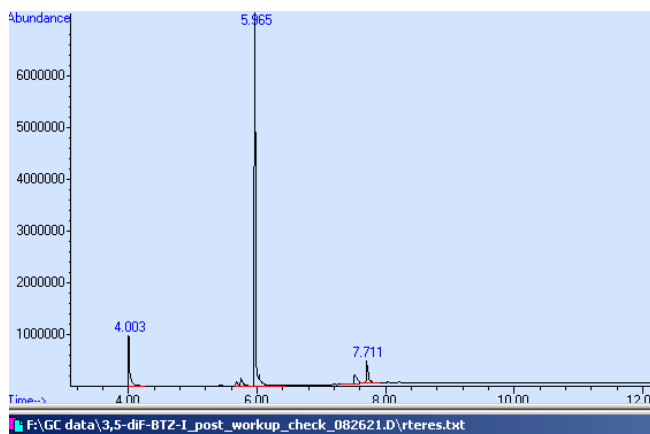

```
Integration Parameters: autoint1.e
Integrator: ChemStation

Method    : C:\msdchem\1\methods\Ketcha\CODY.M
Title     :

Signal    : TIC: 3,5-diF-BTZ-I_post_workup_check_082621.D\data.ms

peak  R.T. first  max last  PK   peak      corr.     corr.    % of
 #    min   scan scan scan  TY  height      area    % max.   total
---  ----- ----- ---- ---- ---  -------   -------   ------  -------
 1   4.003    81   82  106   M  1096582  19945255   21.44%  15.497%
 2   5.965   232  259  301   M  7234729  93008918  100.00%  72.266%
 3   7.711   379  416  435   M2  451498  15748737   16.93%  12.237%
```

Figure 16: GC/MS trace of a 2,4-diF-BTZ-I synthesis and the resulting percentage report

36

Synthesis	Mono-substituted conversion	Di-substituted conversion	Unreacted benzothiazole
1	75.7%	13.2%	11.1%
2	71.2%	21.6%	7.2%
3	70.3%	11.2%	18.5%
4	72.2%	12.2%	15.6%
5	64.6%	30.4%	5%
6	70.6%	26.3%	3.1%
7	51.7%	4.1%	44.2%
8	62.5%	7.4%	30.1%

Table 2: List of 3,5-diF-BTZ-I reactions and their conversion rates

3.3: Synthesis of 2-(3,5-difluorophenyl)-benzothiazole-carbazole, 7

The desired blue emitting chromophore 2-(3,5-difluorophenyl)-benzathiozole-carbazole (3,5-diF-BTZ-CBZ) was successfully prepared using compounds previously synthesized by other group members, following the procedure described by Kemboi, as detailed in section **2.5**. The reaction was monitored via GC/MS, which indicated a conversion of 96.6% to the desired product. The chromophore was purified using recrystallizations from ethanol, and afforded 0.303g, which corresponds to a 36.4% yield. The melting point was determined to be 175°C to 177°C and is consistent with the melting point reported by Kemboi.[19] In the ^{1}H NMR spectrum, the confirming signals are peaks a, c, and d. Peak a corresponds to the proton that is between the two fluorine atoms, which causes it to appear the furthest up-field. Signals from protons c and d have integration values that correspond to a single proton. Peaks f, g, h, and i confirm the presence of the carbazole donor group attached to the benzothiazole.
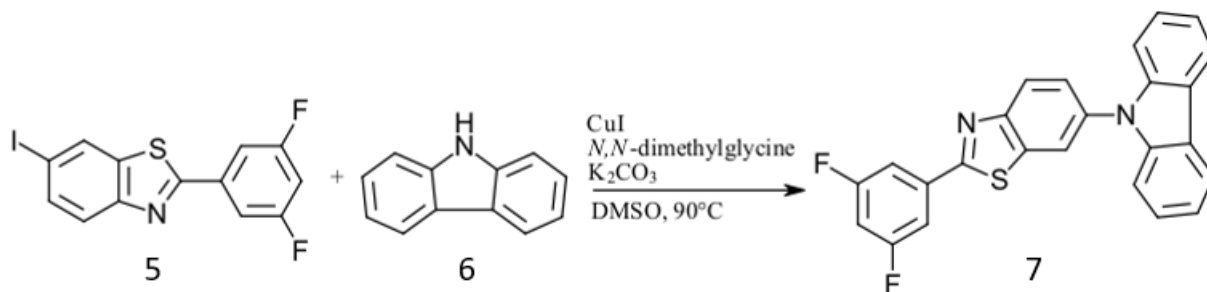
Scheme 12: Synthesis of 3,5-diF-BTZ-CBZ
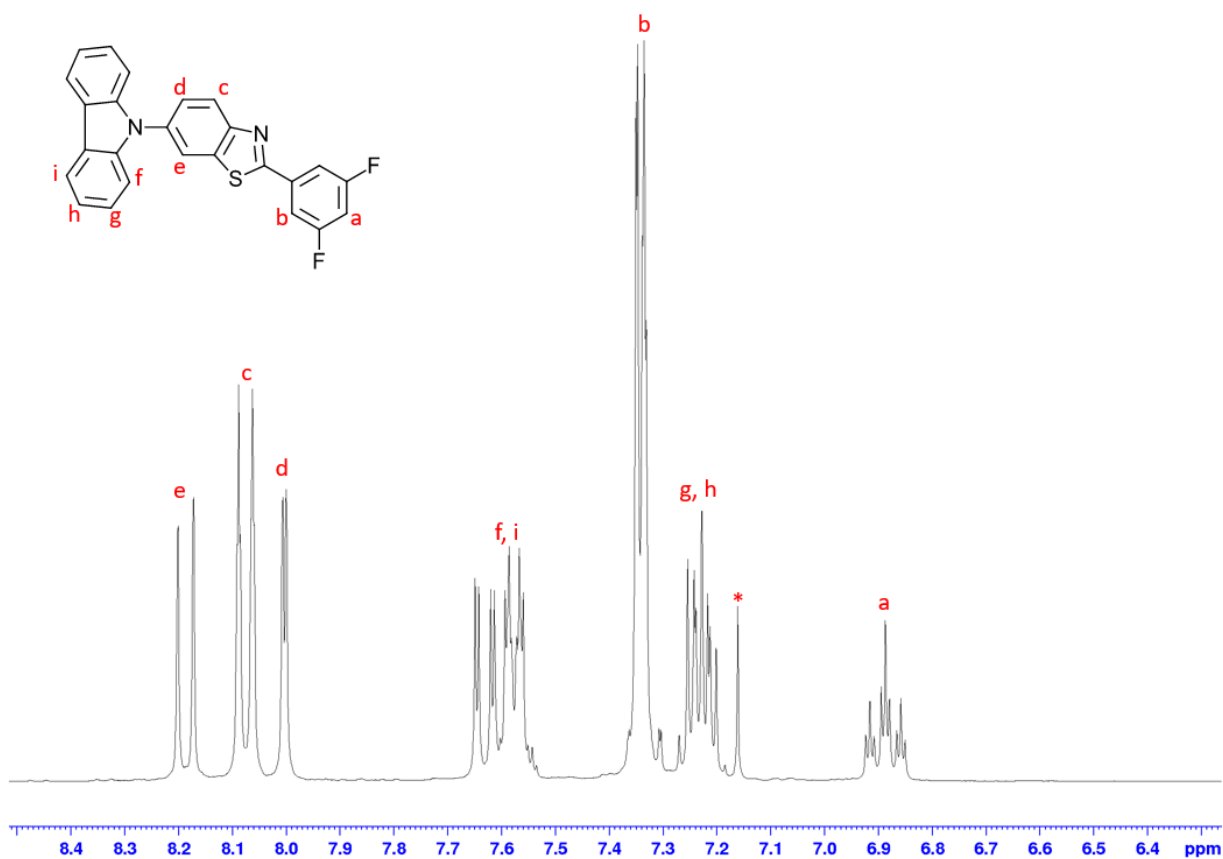
Figure 17: 300MHz ^{1}H NMR spectrum (CDCl$_3$) of 3,5-diF-BTZ-CBZ

3.4: Synthesis of 2-(2,4-difluorophenyl)-benzothiazole, 9

The monomer that served as the electrophilic component for the base polymer, 2-(2,4-difluorophenyl)-benzothiazole (2,4-diF-BTZ) was synthesized following a similar procedure as other benzothiazole syntheses, as detailed in section **2.6**. To an oven dried 250 mL round bottomed flask, 2,4-difluorobenzoic acid (**8**) and **2** were added to PPA and heated at 90°C until the 2,4-difluorobenzoic acid stopped subliming, at which point the temperature was increased to 150°C and left to stir for approximately 12 hours. The reaction was monitored via GC/MS analysis, which confirmed the formation of the desired product. After work-up, 3.25g of a brown/sliver flaky solid was recovered, which corresponds to a 41.2% yield. The melting point was determined to be 104°C to 106°C, which matches previous melting points, reported by Reinhard. The structure of the product was confirmed via ^{1}H NMR. Signals observed from protons d, e, f, and g all integrate to correspond to a single proton, which indicates that the product was successfully synthesized. Also, the signal from proton c is shifted up-field from being between the two fluorine atoms, which further indicated the formation of the product.
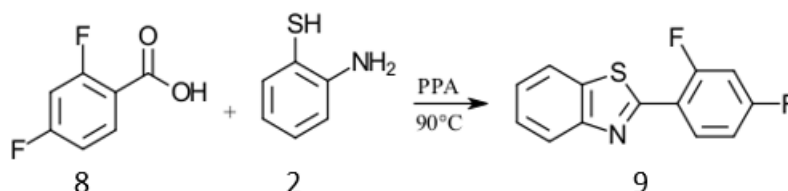
Scheme 13: Synthesis of 2,4-diF-BTZ
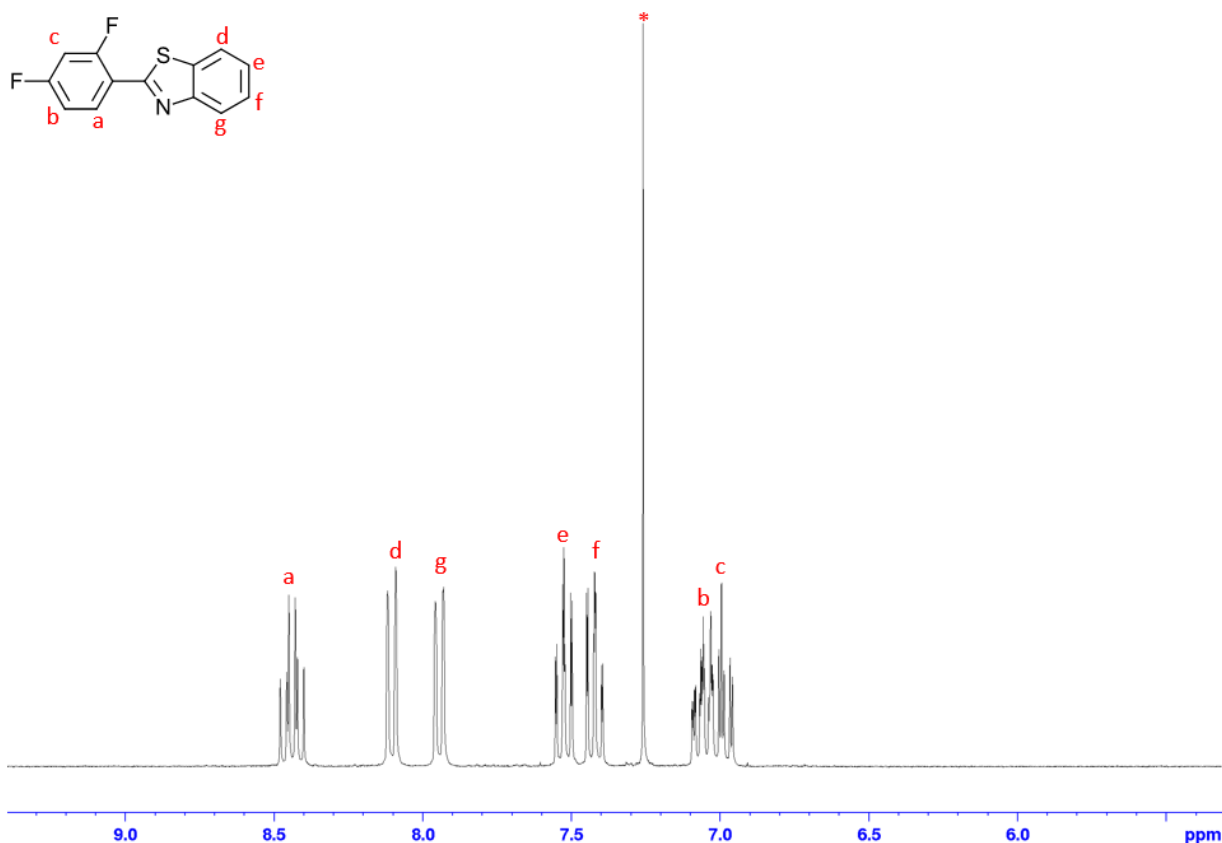
Figure 18: 300MHz ^{1}H NMR of 2,4-diF-BTZ taken by Garrett Reinhard

3.5: Polymerization of 2,4-diF-BTZ and DPE, 11

In synthesized polymers, benzothiazoles act as both the acceptor group of the incorporated chromophore, as well as the electrophilic component of the NAS polycondensation reaction. Polymerizations using **9** and 4,4'-dihydroxydiphenyl ether (**10**) were performed in NMP at a concentration of 0.64M respective to **9,** at 160°C using NAS polycondensation conditions. The reaction was allowed to stir for 24 hours, after which it was precipitated from vigorously stirred water. The resulting solids were isolated via vacuum filtration, and re-precipitated by dissolving in minimal tetrahydrofuran (THF) and added dropwise to a 50:50

mixture of hexanes and 2-propanol (IPA). The reaction afforded a beige powder.

The polymer structure was confirmed via ^{1}H NMR spectroscopy. In the ^{1}H NMR

spectrum, seen in **Figure 19**, there are key changes that are indicative of the

formation of the polymer. Proton c is the best sign, going from a doublet of

triplets in the spectrum of the 2,4-diF-BTZ in **Figure 18** to a doublet in the

polymer spectrum. Other key changes in the spectrum are from protons a and b.

These signals change from a doublet of doublets to a doublet, showing a change

in the coupling coefficients, indicating the loss of coupling to the fluorines that are

displaced. The peaks were assigned based on the integrations. Peaks a, b, c, d,

e, f, and g all had integration values of one, indicating that those peaks

correspond to a single proton, while peaks h and i had integrations that were

greater than one, corresponding to several identical protons in the DPE

component. The integrations values of peaks h and i do not add to four protons.

This is accounted for by the various connections that occur in the polymer. The

DPE component can attach to the benzothiazole in three different configurations:

at the 2,2 position, 2,4 position and the 4,4 position, resulting in the two observed

peaks.
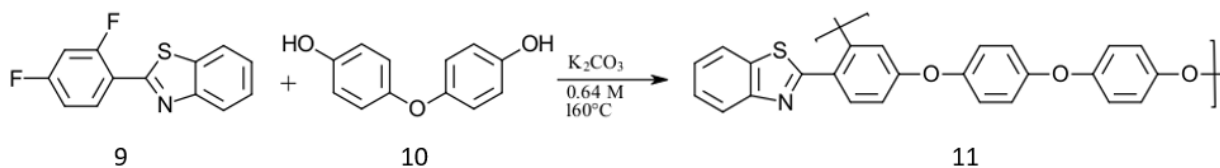
Scheme 14: Synthesis of 2,4-diF-BTZ-DPE polymer
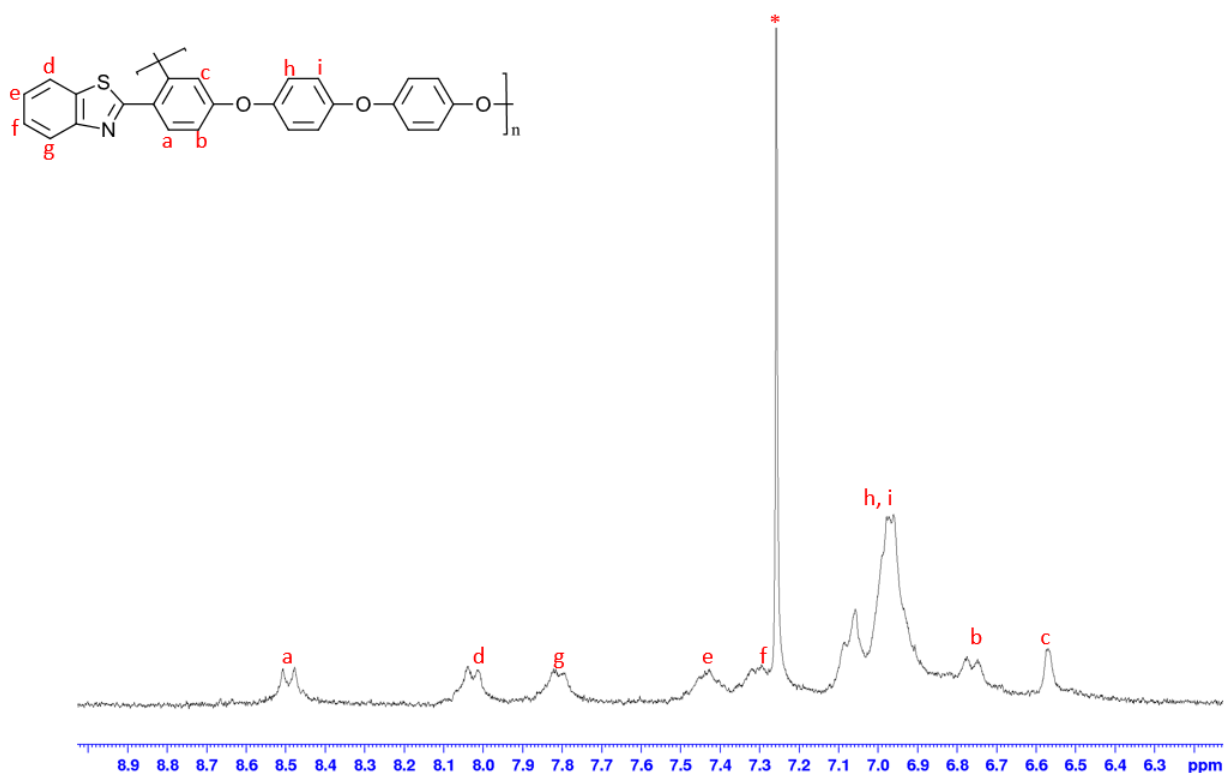
Figure 19: 300 MHz ^{1}H NMR spectrum (CDCl$_3$) of 2,4-diF-BTZ-DPE polymer

While the synthesis of polymer **11** afforded relatively high molecular weight materials, the NMR spectrum indicated the presence of additional products with very similar signal patterns. As can be seen in **Figure 19**, there are some additional lower intensity signal signals present, for example, the peaks at 8.65 ppm have the same coupling constant as the peaks at 8.5 ppm. There are two possibilities to explain the addition peaks. First, the reaction could be incomplete, and the peaks are indicative of polymer end groups, which would be more easily observed at low molecular weights. A second possibility is the formation of low molecular weight, cyclic species. Alongside the formation of the polymer, the reaction also forms cyclic byproducts, which limits the yield of the reaction. The presence of the cyclics is indicated by sharp peaks observable in

the NMR spectrum seen on **Figure 19**. Since the reaction was run for a considerable amount of time the formation of cyclics species was the more likely explanation.

In an attempt to correct this issue, the reaction was done again, with the DPE being added in three portions, the first containing 50% of the total mass of DPE and two containing 25% each. The larger portion was added at the start of the reaction and the two smaller portions were added separately after 24 hours and 48 hours. This attempted to have the end groups of the polymer to be the same monomer unit, which prevents cyclics from forming, since two of the same monomer groups will not attach to one another. This reaction had some success in limiting the amount of cyclic by-products formed but did not completely eliminate the formation.

The separation of the cyclic byproducts was facilitated through a precipitation of the polymer in the 50:50 hexanes and IPA mixture. The smaller cyclic structures are more soluble in the mixture. A higher weight polymer offers a smaller change in entropy than smaller molecular weight polymers. This places a solubility limit on the polymer, which prevents the higher molecular weight polymer from dissolving and causes the smaller cyclic structures to be more soluble. This process was applied to the product from the original polymerization reaction.
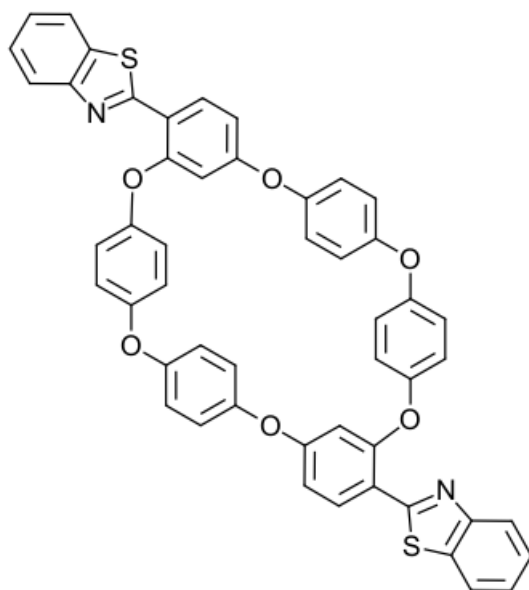
Figure 20: Smallest possible structure for the cyclic by-products

The formation of the cyclic by-products was confirmed by another synthesis designed to purposefully make the by-products. This reaction was run in dilute conditions. The concentration respective to **9** was decreased to $6.4*10^{-5}$ M, and the mass used of each starting material reduced by a factor of 5 and the volume of NMP doubled. The formation of cyclics was favored in this reaction due to the low interactions between separate polymer chains. The end groups would circle around until it met the other end group and attach, forming the cyclic structure. The ^{1}H NMR spectrum confirmed that the cyclic by-products were successfully synthesized and show a difference from the polymer. **Figure 21** shows the difference in the NMR spectra acquired from .three different samples: purposely made cyclics, polymer without the cyclics removed and polymer with the cyclics removed. At 6.55 ppm, in the two polymer samples, a singlet can be

seen that is absent in the purposely made cyclic sample. At 7 ppm, a doublet is observed in the spectra for the purposely made cyclics and the polymer without the cyclics removed. At 7 ppm, in the purposely made cyclics, a multiplet is observed, as compared to a doublet observed in the other two samples. In the two samples of polymer, a doublet at 6.75 ppm and 8.5 ppm is observed, which is absent in the sample of just cyclics. The final notable difference between the samples is a signal at 8.65 ppm that is observed in the sample of cyclics and the polymer without the cyclics removed that is not observed in the sample with the cyclics removed.
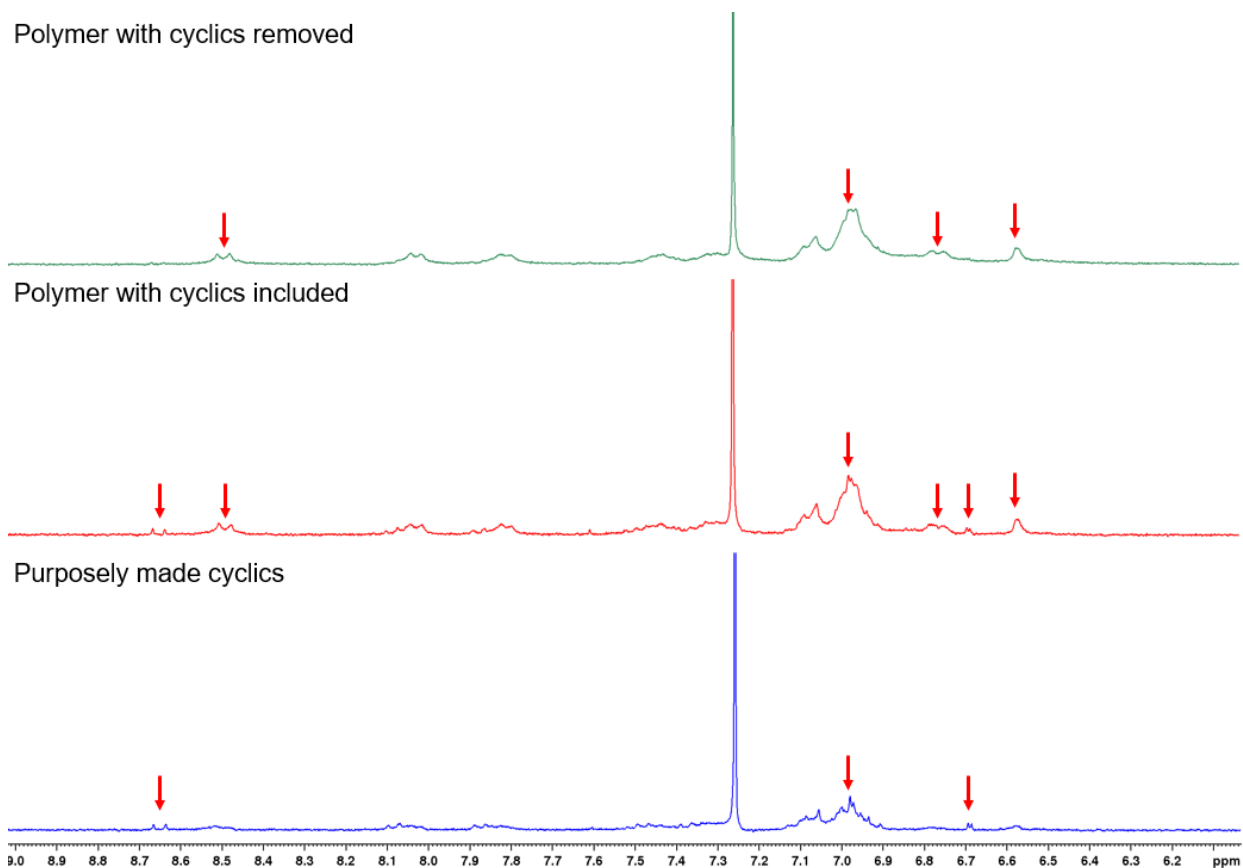
Figure 21: Stacked 300 MHz ^{1}H NMR spectra of a sample of purposely made cyclics by-products, polymer without the cyclics removed and polymer with the cyclics removed

Thermal analysis of polymer **11** was done to evaluate its thermal properties. Differential scanning calorimetry (DSC) was performed to find the glass transition temperature (T_g) of the polymer. DSC samples were heated to 300°C and revealed only a T_g, indicating that the polymer was completely amorphous. The T_g was found to be 144°C, measured at the inflection point of the signal seen in the DSC trace in **Figure 22**.
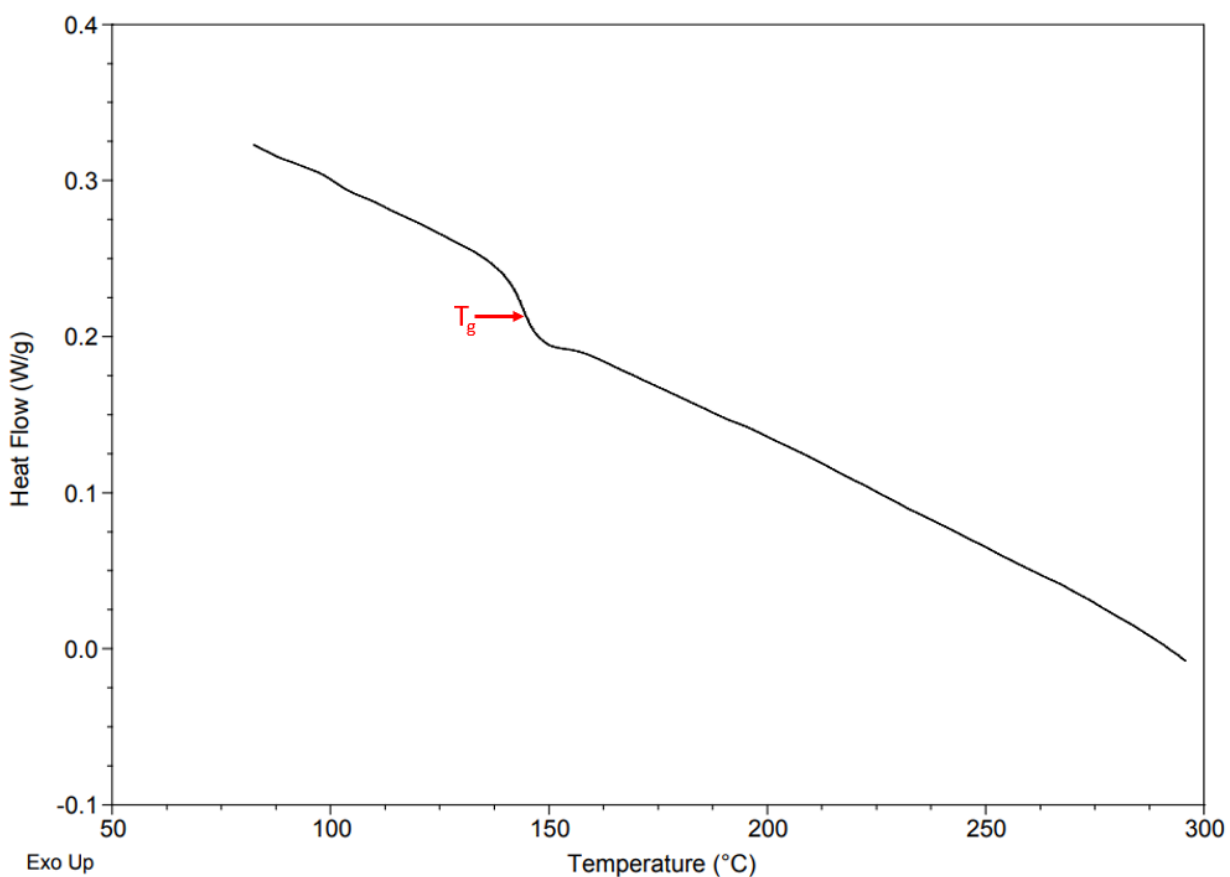
Figure 22: DSC trace of 2,4-diF-BTZ-DPE

3.6: Synthesis of 2,4-diF-BTZ-BP polymer, 13

Since the flexible bisphenol **10** gave rise to difficulties in preparing high
molecular weight materials, along with the formation of cyclic species, an
alternative and more rigid bisphenol, 4,4'-biphenol (**12**) was utilized.
Polymerizations using **9** and **12** were performed in NMP at a concentration of
0.64M respective to **9**, at 160°C using a NAS polycondensation conditions. The
reaction was allowed to stir for 24 hours, at which point it was precipitated from
vigorously stirred water. The resulting solids were isolated via vacuum filtration,
and re-precipitated by heating in toluene, then dissolving in minimal chloroform.

The solution was added dropwise to a 50:50 mixture of hexanes and IPA, which afforded a tan powder. The polymer structure was confirmed via ^{1}H NMR spectroscopy. The ^{1}H NMR spectrum, seen in **Figure 23**, showed several key changes that indicated the formation of the polymer. The signal from proton g changed from a doublet of triplets to a singlet. The signals from protons e and f changed from a doublet of doublets to doublets. The assignments were done through the integration of the spectrum. Protons a, b, c, d, e, f, and g all have integrations of one, indicating that those signals all come from one proton. The integrations of protons h and i have integrations larger than one, which corresponds to their position on the biphenol.
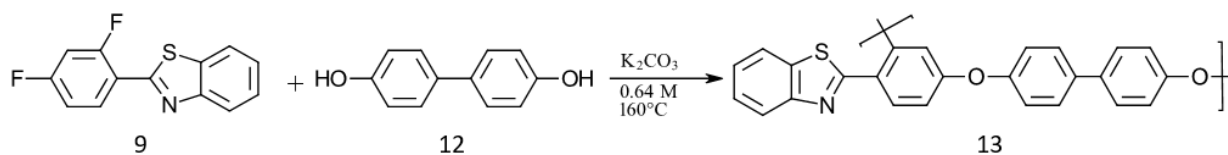
Scheme 15: Synthesis of 2,4-diF-BTZ-BP polymer
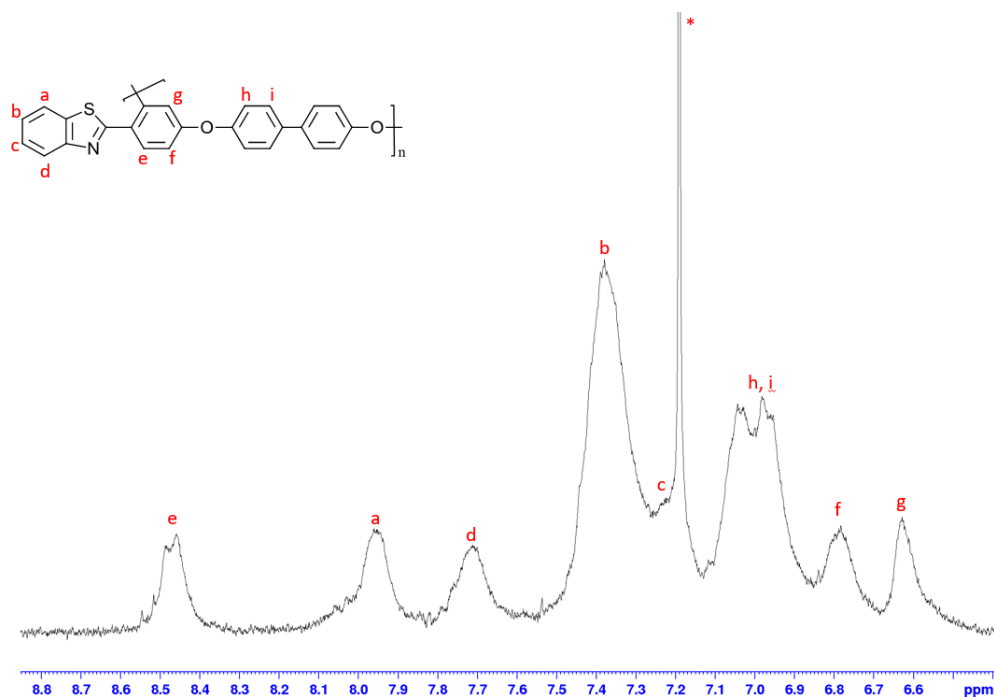
Figure 23: 300 MHz ^{1}H NMR of 2,4-diF-BTZ-BP polymer

Thermal analysis of polymer **13** was done to evaluate the thermal properties. DSC was performed to find the T_g of the polymer. DSC samples were carried to a temperature of 300°C and revealed only a T_g, indicating that the polymer was completely amorphous. The T_g was found to be 146°C, as measured at the inflection point of the signal seen in the DSC trace in **Figure 24**.
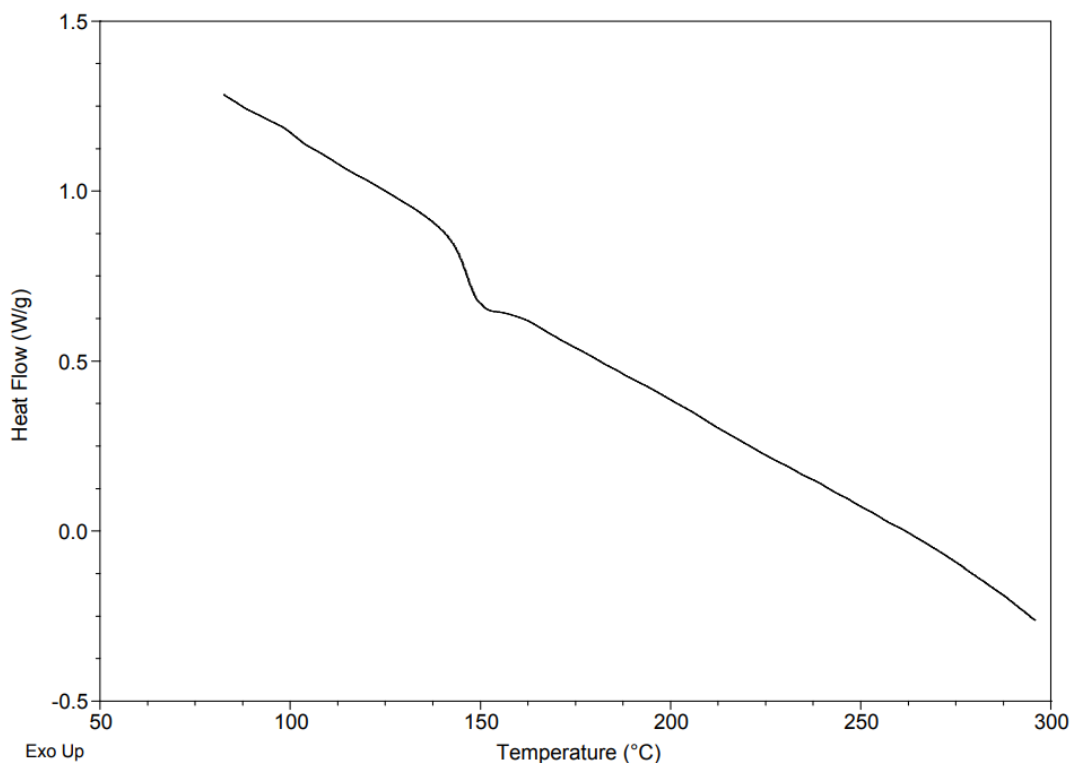
Figure 24: DSC trace of 2,4-diF-BTZ-BP polymer

3.7: Synthesis of Chromophore Containing Copolymers

Copolymers, made with 10% of the chromophore, **7**, made using **9** and **11** were done in NMP at a concentration 0.64M respective to **9,** at 160°C using NAS polycondensation conditions. In copolymer syntheses, a 10% molar equivalence of **9** was replaced by a 10% molar equivalent of chromophore **7**, while the bisphenol was held constant. After 24 hours, the reaction was precipitated from vigorously stirred water and the resulting solids were isolated via vacuum filtration. The solids were then dissolved in minimal chloroform and re-precipitated from a 50:50 mixture of hexanes and IPA, which afforded a brown powder. The copolymer structure was confirmed using ^{1}H NMR spectroscopy.

50
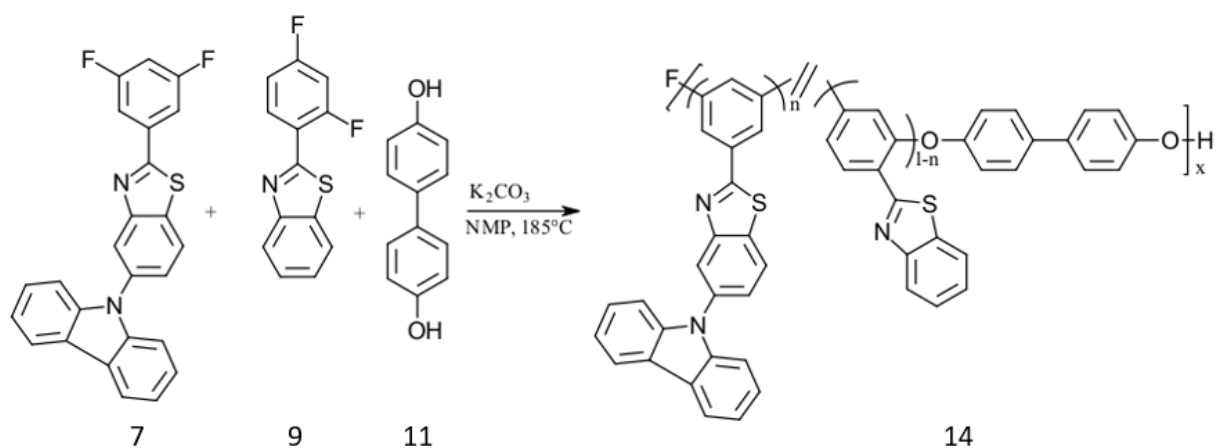
Scheme 16: Reaction scheme of the formation of the 3,5-diF-BTZ-CBZ 2,4-diF-
BTZ/BP

The initial attempt of this reaction was only partially successful. When
stirred at 160°C, only one fluorine in compound **7** is able to be displaced, limiting
the molecular weight of the polymer. The limitations on the molecular weight
when only one fluorine is displaced follows the Carother's equation, $DP = \frac{1}{1-p}$, or

$DP = \frac{1+r}{1-r}$. In the partially displaced copolymer, 10% of the 2,4-diF-BTZ is being

replaced by 3,5-diF-BTZ-CBZ, however, since only one fluorine is displaced, the

percentage of 3,5-diF-BTZ-CBZ is actually only 5%. When put into Carother's

equation, this results in a R value of .95, which causes the degree of

polymerization to be a maximum of 20. In the fully displaced polymer, the 3,5-

diF-BTZ-CBZ is fully incorporated, with a p or r value of .99, which results in a

degree of polymerization of 100. This causes the difference in the molecular

weights of the two copolymers. Extra peaks seen in the ^{1}H NMR spectrum

indicate that the chromophore was not fully displaced under the reaction

conditions. Previous polymerizations done by Kemboi incorporating chromophore **7** into a polymer were heated at 185°C to fully incorporate the chromophore. In an attempt to displace the second fluorine, the temperature was increased to 185°C for another 24 hours. Unfortunately, the increased reaction temperature resulted in an insoluble material, at least in any typical PAE solvents, such as NMP, chloroform and THF. One possible explanation for the insoluble nature might be that the polymer was slightly crosslinked due to a side reaction, but further work is necessary for a definitive answer. To address the solubility issues, compound **7** was polymerized first, stirred at 185°C for 24 hours, at which point compound **9** was added, and the temperature was dropped to 160°C to complete the polymerization. This also resulted in material that exhibited poor solubility characteristics. Another reaction was run, with compound **7** being polymerized first again, this time at 160°C for 24 hours, then compound **9** was added, and the reaction was left to stir for another 24 hours. The resulting polymer was soluble in NMP, as well as in THF and chloroform, indicating that the lower reaction temperature successfully inhibited any side reactions. The reaction at 160°C was successful due to the low reactivity at lower temperatures being overcome by reacting **7** with an excess of bisphenol, which causes the kinetics to be in favor of the displacement of both fluorine atoms in a reasonable amount of time. The polymer structure was confirmed via ^{1}H NMR spectroscopy. The spectrum seen in **Figure 25** is of the partially displaced copolymer. The largest indication that the copolymer was formed is the increase in the peak seen at 7.45 ppm. This peak has an integration value that corresponds to six protons, most found on the

carbazole donor group. Other key changes in the spectrum that indicate the formation of the copolymers is peak a changing from a doublet of triplets into a singlet, as well as signals from protons m, f and q shifting from a doublet of doublets into a doublet and singlets. The spectrum seen in **Figure 26** shows the ^{1}H NMR spectrum of the fully displaced copolymer. This spectrum is similar to the spectrum of the partially displaced copolymer and share the same indications as the partially displaced copolymer. The signal from protons c and l have blended together since their conditions have become the same, with the protons being in between two polymerization sites the form ether bonds. Chromophore incorporation is confirmed by the increase of the integration value of the peak seen at 7.45 ppm, as well as the ^{1}H NMR samples made fluorescing blue when exposed to UV light.
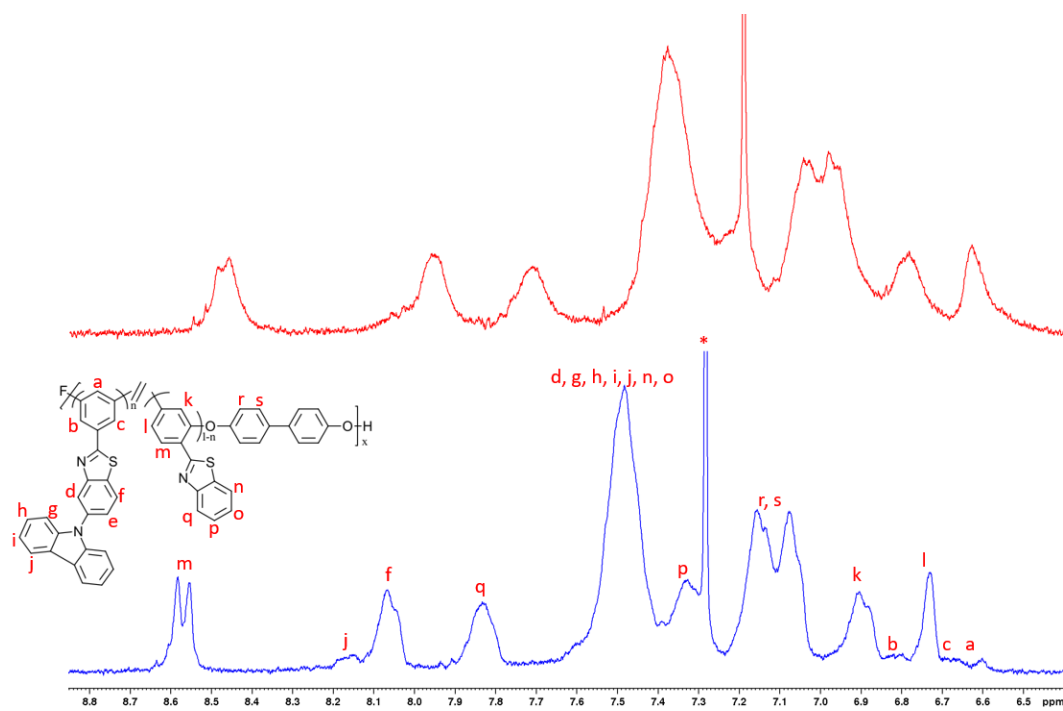
Figure 25: 300 MHz ^{1}H NMR of 3,5-diF-BTZ-CBZ 2,4-diF-BTZ/BP partially displaced copolymer stacked with the ^{1}H NMR spectrum of the base polymer
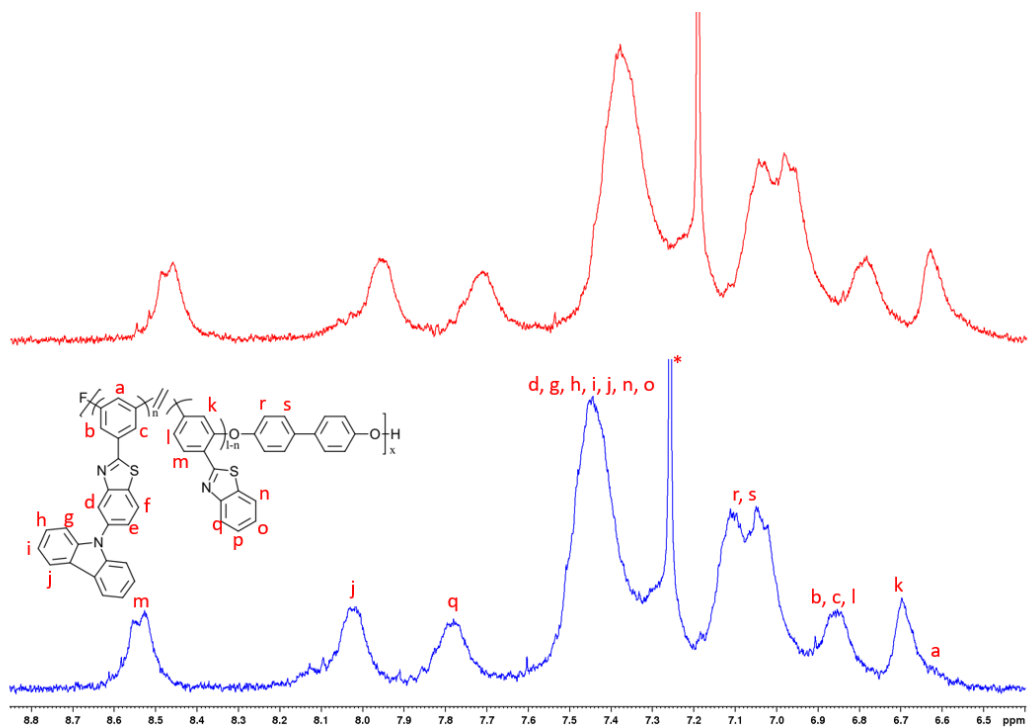
Figure 26: 300 MHz ^{1}H NMR of the fully displaced copolymer stacked with the ^{1}H NMR spectrum of the base polymer

Thermal analysis of the various copolymers prepared under different conditions was performed to determine the presence of any thermal transitions. In the DSC traces, shown in **Figure 27**, only one transition, a T_g, was observed. The traces were taken to a temperature of 300°C and indicated that the copolymers were completely amorphous. The partially displaced copolymer had a T_g of 203.3°C, while the fully displaced copolymer had a T_g of 223.3°C. When compared to the base 2,4-diF-BTZ base polymer, the incorporation of the chromophore increased the T_g significantly. In the mono-substituted copolymer, the T_g increased by 57.3°C. The T_g of the fully displaced copolymer increased 77.3°C.
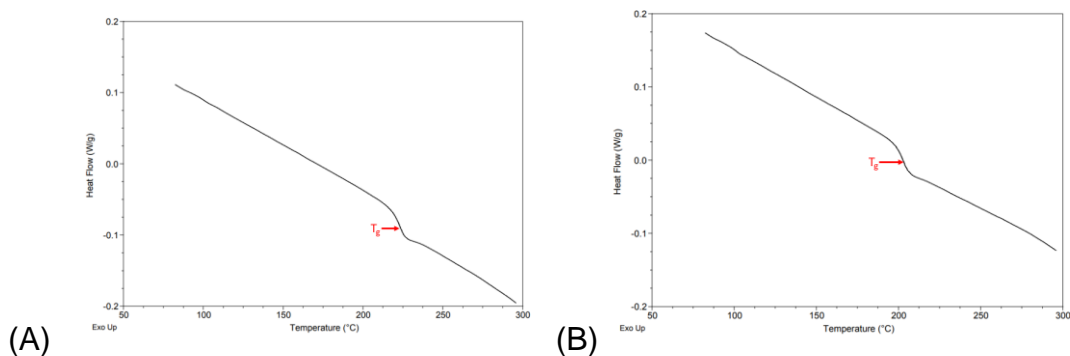
Figure 27: DSC traces of (A) the fully displaced copolymer and (B) the partially displaced copolymer

3.8: Absorption and emission of copolymers

UV/Vis spectroscopy was used to find the absorbance spectrum of polymer **11** and **14**. Polymer **11** showed weak absorption in the UV range, with a peak absorbance at 284 nm. The absorbance spectrum can be seen in **Figure 28a**. An absorbance peak is also observed at a longer wavelength at 325 nm. Fluorescence spectroscopy was also performed to confirm the incorporation of the chromophore into the base polymer. The base polymer had no emission and neared the dark limit of the monochromator as the wavelength increased. The emission spectrum can be viewed in **Figure 28b**.
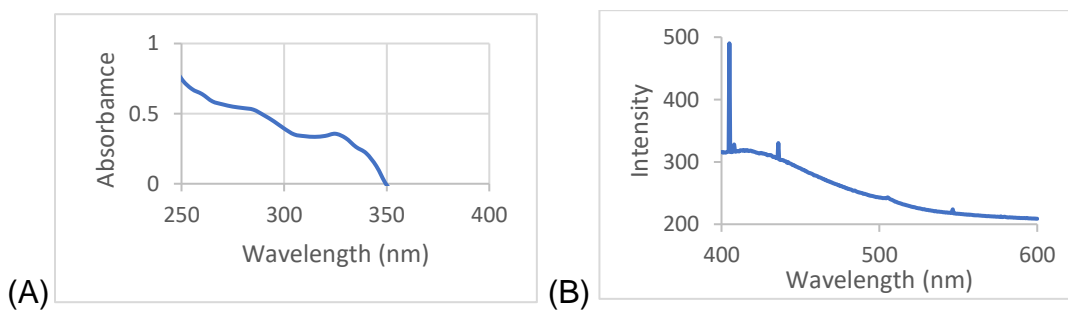
UV/Vis analysis was also performed on copolymer **14**, as well as the monomers. The absorbance spectra can be seen in **Figure 29**. When compared to each other, the copolymer has a much stronger absorption than the base polymer, with a peak absorbance at 278 nm. Another absorbance peak for the copolymer can be seen at 327 nm. When compared to the monomers, the absorbance of the copolymer is much stronger than the monomers, and absorbs different wavelengths of light, with the 2,4-diF-BTZ having a peak absorbance at 285 nm and the 4,4'-biphenol having a peak absorbance at 280nm. Both of the monomers had weak absorbances. When compared to the base 2,4-diF-BTZ-BP polymer, the absorbance is stronger in the copolymer, indicating the addition of the chromophore increases the absorbance. Discrepancies where the signal observed in the spectra go below zero are due to an internal instrument error.
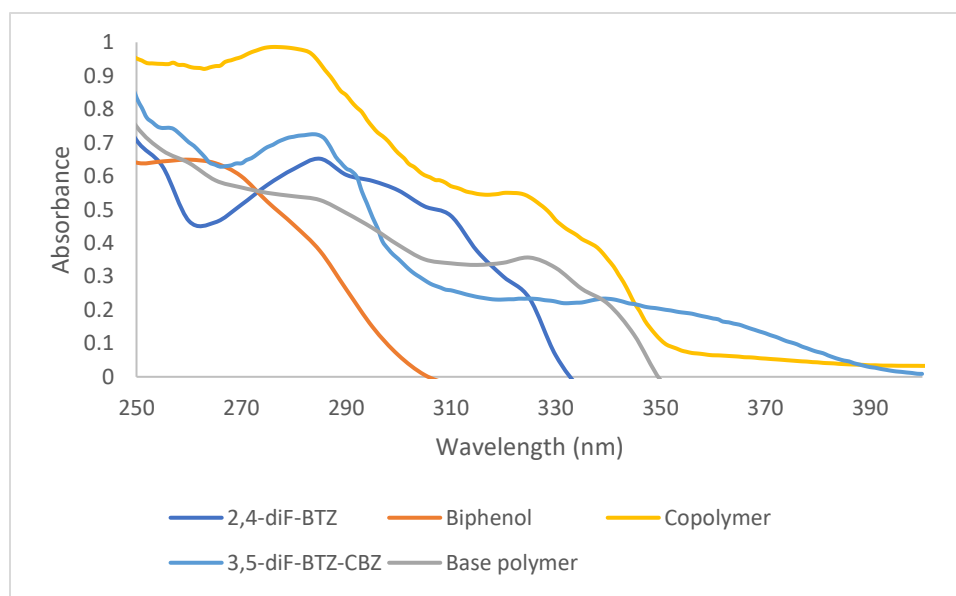
Figure 29: UV/Vis spectrum of the 3,5-diF-BTZ-CBZ 2,4-diF-BTZ/BP copolymer, 2,4-diF-BTZ-BP base polymer, and 2,4-diF-BTZ and 4,4'-biphenol monomers

Copolymers were taken up in THF, and excited using a Spectroline ultraviolet lamp at 365 nm and the light was directed into a monochromator. The fully displaced copolymer had a peak emission of 471 nm. The emission spectrum can be seen in **Figure 30a**. The sharp peaks that are can be seen at 405 nm, 406 nm and 436 nm are all mercury emission lines that are from the UV lamp. The partially displaced copolymer had a peak emission of 493.5 nm. The emission spectrum can be seen in **Figure 30b**. This is considerably red shifted compared to the fully displaced copolymer. This may be due to the additional electron donations given by the connection to the 4,4'-biphenol monomer unit. The color of the sample shifted from colorless to yellow after the emission data was collected, most likely caused by phenol end groups oxidizing. The solvent that the samples were analyzed in also play a role in the observed signals, due to solvatochromism. A more polar solvent causes the emitted light to be more red shifted , while a nonpolar solvent causes the light to blue shift.

(A) (B)
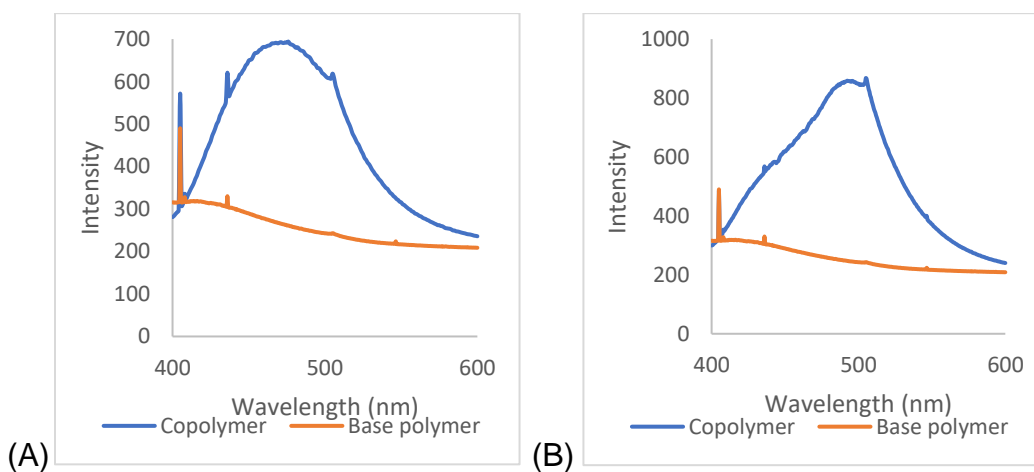
Figure 30: Fluorescence emission of (A) 3,5-diF-BTZ-CBZ 2,4-diF-BTZ/BP fully displaced copolymer and (B) 3,5-diF-BTZ-CBZ 2,4-diF-BTZ/BP partially displaced copolymer overlayed with the base polymer

One indication of that the molecular weight of the copolymers is above the chain entanglement length is the ability to cast films. Both copolymers were able to cast into a film. Films that were cast of the copolymers were excited at 365 nm using a TLC lamp. The films were brittle and fragile and could not be handled with anything other than forceps or could not be removed from the glass slide that it was cast on. When excited, the light emitted by the films is blue to the eye.
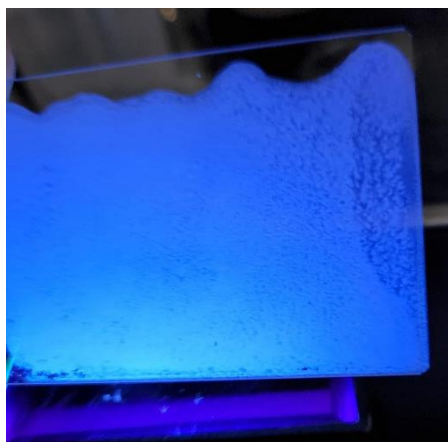
Figure 31: Film cast of the partially displaced 3,5-diF-BTZ-CBZ 2,4-diF-BTZ/BP copolymer

4. Conclusions

The benzothiazoles needed for polymer synthesis were successfully synthesized with acceptable yields and excellent purity. The identities of the compounds were confirmed with GC/MS analysis and NMR spectroscopy. The synthesis of 3,5-diF-BTZ-I was proved difficult, as the reaction formed both the desired mono-substituted product and di-substituted byproduct, which couldn't be removed completely, the di-substituted byproduct, with the lowest percentage of the di-substituted material achieved was 3%. The synthesis of the complete 3,5-diF-BTZ-CBZ was successful using materials that were previously made be other group members. The formation of the chromophore was confirmed using GC/MS analysis and NMR spectroscopy, while its purity was determined by melting point.

Polymer syntheses were accomplished via NAS polycondensation reactions using either 4,4'-dihyrdoxydiphenyl ether, DPE, or 4,4'-biphenol, BP. The synthesis of 2,4-diF-BTZ-DPE provided relatively high molecular weight material and the structure was confirmed using NMR spectroscopy. However, the formation of cyclic byproducts significantly reduced the yield of the reaction. The T_g of the polymer was determined to be 144°C, determined via DSC. The synthesis of 2,4-diF-BTZ-BP was considerably more successful, with a high yield of polymer, and a limited formation of cyclic species due to the more rigid

characteristics of the BP monomer. The structure of the polymer was confirmed using NMR spectroscopy. The T_g of the polymer was found using DSC and was determined to be 124°C.

Incorporation of the 3,5-diF-BTZ-CBZ chromophore was successful, and two different copolymers were made, both containing 10 mole% of the chromophore. In the first copolymer, only one of fluorine on the chromophore was displaced, which limited the molecular weight of the polymer. In the second copolymer, both fluorines on the chromophore were successfully displaced. The structure of the copolymers was confirmed using NMR spectroscopy. The glass transition temperature of the copolymers was determined using DSC. Both copolymers had a T_g over 200°C, with the partially displaced copolymer exhibiting a T_g of 203°C, while the fully displaced copolymer had a T_g of 223.3°C. Unfortunately, films cast of the copolymers were fragile and brittle.

UV/Vis and fluorescence spectroscopy was performed to find the absorption and the emission wavelengths of the copolymers. The copolymers had the same peak absorption at 278 nm. In a THF solution, the partially displaced copolymer had a broad emission, spanning from 400 nm to 600 nm, with a peak emission at 494 nm; an excitation wavelength of 365 nm was utilized. The fully displaced copolymer also had a broad emission, spanning again from 400 nm to 600 nm, with a peak emission at 471 nm.

5. Future Work

Current research has determined that it is possible to covalently attach the 3,5-diF-BTZ-CBZ chromophore to a host polymer and that the polymer will successfully fluoresce when excited. Other host polymers should be explored to find copolymers that do not form fragile films. More spectral data also should be collected to find the copolymers exact excitation wavelength, as well as the photophysical work to determine the effect the host polymer has on the efficiency of the chromophore and triplet state energies of the host material. More thermal analysis should be performed on the current copolymers and future polymers to find the 5% weight loss temperature. Gel permeation chromatography should also be performed to find the exact molecular weight and chain length of synthesized polymers.

6. References

(1)   How Energy-Efficient Light Bulbs Compare with Traditional Incandescents.

.   https://www.energy.gov/energysaver/save-electricity-and-fuel/lighting-choices-save-youmoney/how-energy-efficient-light. (accessed: 4/4/2022)

(2)   *Energy efficient light bulbs. [electronic resource] : a bright idea.* Federal Trade

Commission, Bureau of Consumer Protection, Office of Consumer and Business

Education: 2000.

(3)   Gillessen, K.; Schairer, W., *Light emitting diodes: an introduction.* Prentice/Hall

International: 1987.

(4)   Kappaun, S.; Slugovc, C.; List, E. J. W. Phosphorescent Organic Light-Emitting

Devices: Working Principle and Iridium Based Emitter Materials. *Int. J. Mol. Sci.*

August 2008, pp 1527–1547.

(5)   Im, Y.; Kim, M.; Cho, Y. J.; Seo, J. A.; Yook, K. S.; Lee, J. Y. Molecular Design

Strategy of Organic Thermally Activated Delayed Fluorescence Emitters. *Chem.*

Mater. American Chemical Society March 14, 2017, pp 1946–1963.

(6)   Volz, D., Review of organic light-emitting diodes with thermally activated delayed

fluorescence emitters for energy-efficient sustainable light sources and displays.

Journal Of Photonics For Energy 2016, 6(2), 020901.and Displays. *Journal of Photonics for Energy* **2016**, *6* (2), 020901-1-020901-13

(7)   Kondakov, D. Y.; Pawlik, T. D.; Hatwar, T. K.; Spindler, J. P. Triplet Annihilation Exceeding Spin Statistical Limit in Highly Efficient Fluorescent Organic Light- Emitting Diodes. *J. Appl. Phys.* **2009**, *106* (12), 124510-1-124010-7

(8)   Youn Lee, S.; Yasuda, T.; Nomura, H.; Adachi, C. High-Efficiency Organic Light-Emitting Diodes Utilizing Thermally Activated Delayed Fluorescence from Triazine-Based Donor-Acceptor Hybrid Molecules. *Appl. Phys. Lett.* **2012**, *101*, 093306-1-093306-4

(9)   Lee, I.; Lee, J. Y. Molecular Design of Deep Blue Fluorescent Emitters with 20% External Quantum Efficiency and Narrow Emission Spectrum. *Organic Electronics* **2016**, *29*, 160–164.

(10)   Wei, Q.; Ge, Z.; Voit, B. Thermally Activated Delayed Fluorescent Polymers: Structures, Properties, and Applications in OLED Devices. *Macromol. Rapid Commun.* **2019**, *40*, 1800570-1-1800570-19

(11)   Burroughes, J. H.; Bradley, D. D. C.; Brown, A. R.; Marks, R. N.; Mackay, K.; Friend, R. H.; Burns, P. L.; Holmes, A. B., Light-emitting diodes based on conjugated polymers. *Nature* 1990, 347, 539-541.

(12)   Xie, Y.; Li, Z. Thermally Activated Delayed Fluorescent Polymers. *Journal of Polymer Science, Part A: Polymer Chemistry*. John Wiley and Sons Inc. February 15, 2017, pp 575–584.

(13) Nikolaenko, A. E.; Cass, M.; Bourcet, F.; Mohamad, D.; Roberts, M. Thermally Activated Delayed Fluorescence in Polymers: A New Route toward Highly Efficient Solution Processable OLEDs. *Adv. Mat.* **2015**, *27* (44), 7236–7240.

(14) Nobuyasu, R. S.; Ren, Z.; Griffiths, G. C.; Batsanov, A. S.; Data, P.; Yan, S.; Monkman, A. P.; Bryce, M. R.; Dias, F. B. Rational Design of TADF Polymers Using a Donor-Acceptor Monomer with Enhanced TADF Efficiency Induced by the Energy Alignment of Charge Transfer and Local Triplet Excited States. *Adv. Optical Mater.* **2016**, *4* (4), 597–607.

(15) Zhang, Y.; Wang, S.; Wang, Z.; Gai, S.; Song, X. M. Preparation and Performance of Crosslinked Poly(Arylene Ether)s Containing Azobenzene Chromophores. *Designed Monomers and Polymers* **2017**, *20* (1), 496–504.

(16) Fetters, H., Functionalized PEEK Analogues from 2,4- and 3,5- Difluorobenzophenone Derivatives. Wright State University/OhioLINK: 2019.

http://rave.ohiolink.edu/etdc/view?acc_num=wright1559497023409191

(17) Smith, J. G. In *Organic Chemistry.* Fourth ed.; McGraw-Hill, New York, NY, 2014, 695-699

(18) Picker, J. L*., Routes to N-Heterocycle Functionalized Poly(arylene ether sulfone)s.* Wright State University/OhioLINK: 2014. http://rave.ohiolink.edu.ezproxy.libraries.wright.edu/etdc/view?acc_num=wright14 09597 075

(19)   Kemboi, A. K., *Design and Application of Facile Routes to N-Heterocycle Functionalized Poly(arylene ether)s.* Wright State University/OhioLINK: 2016. http://rave.ohiolink.edu.ezproxy.libraries.wright.edu/etdc/view?acc_num=wright14 64120 801

(20)   Slaybaugh, A., *Structure-Property Relationships In PAEs Prepared From 2-(2,4-difluorophenyl)benzoxazole Derivatives*. Wright State University/OhioLINK: 2018. http://rave.ohiolink.edu.ezproxy.libraries.wright.edu/etdc/view?acc_num=wright15 26553 989709853